ADVANCED THERAPEUTICS
www.advtherap.com

Broad Scale and Structure Fabrication of Healthcare Materials for Drug and Emerging Therapies via Electrohydrodynamic Techniques

*Prina Mehta, Aliyah Zaman, Ashleigh Smith, Manoochehr Rasekh, Rita Haj-Ahmad, Muhammad S. Arshad, Susanna van der Merwe, M.-W. Chang, and Z. Ahmad**

The engineering of advanced healthcare materials provides a platform to address challenges facing interdisciplinary scientists, clinicians, pharmacists, biomaterial scientists, and biomedical engineers. Niche, timely developments arising from the synthesis or extraction of more biocompatible materials, new biologically active components, clearer insights into disease mechanisms, and novel therapies provide several timely opportunities. These include enhanced therapies with greater patient compliance, improved disease targeting, better diagnosis, and bespoke medications for individuals. Electrohydrodynamic atomization (EHDA) comprises several processes making use of electric fields interplaying with several forces. Coupled to advanced materials and specifically configured apparatuses, effective and controlled fabrication of various structures on various scales possessing various dimensions is readily achieved. The processes have distinct advantages compared to established engineering methods (ambient environment engineering, low shear, scalability, compartmentalization, etc.). This detailed review focuses on key concepts and developments in EHDA engineering pertaining to underlying principles, enabling tools and engineered structures specifically for healthcare remits. From initial experiments involving the behaviour of non-formulated liquids on charged amber to recent developments in complex 3D matrix printing, the EHDA route has progressed significantly in the last two decades, and is capable of providing timely platform opportunities to tackle several global healthcare challenges.

1. Introduction

In recent years, there has been exponential growth in the field of nanotechnology and biomedical engineering with respect to research and development. The increased interest in the production of micro- and nanometer scaled structures has allowed ground breaking developments to occur both in the pharmaceutical industry and healthcare sector. Multifunctional structures with complex kinetics have great potential within the pharmaceutical and drug-delivery (DD) remits acting as drug carriers, tissue scaffolds in biomaterial engineering, or markers in imaging.

Crucial developments in DD have transformed existing methods, eliminating drawbacks associated with traditional approaches. The processing conditions of more conventional methods for the production of multifactorial particles can induce product degradation, resulting in the nature or function of the active being compromised.[1,2]

Electrohydrodynamic atomization (EHDA), as of late, has been shown to be a versatile technique with abundant potential in DD and bioengineering.[3] The fundamental principle revolves around using electrical forces to atomize liquids (or bespoke formulations) for the production of micro- or nanostructures suitable for various branches in DD. As a result, it has attracted the attention of scientists from various engineering and physical science disciplines. Congenitally, these comprise one-step processes that can be employed at

Dr. P. Mehta, A. Zaman, Dr. M. Rasekh, Dr. R. Haj-Ahmad,
Dr. M. S. Arshad, Prof. Z. Ahmad
Leicester School of Pharmacy
De Montfort University
Leicester LE1 9BH, UK
E-mail: zahmad@dmu.ac.uk

Dr. A. Smith, Dr. S. Van Der Merwe
School of Pharmacy and Biomedical Sciences
St. Michael's Building
University of Portsmouth
White Swan Road, Portsmouth PO1 2DT, UK

Dr. M.-W. Chang
College of Biomedical Engineering and Instrument Science
Zhejiang University
Hangzhou 310027, China

Dr. M.-W. Chang
Zhejiang Provincial Key Laboratory of Cardio-Cerebral Vascular Detection Technology and Medicinal Effectiveness Appraisal
Zhejiang University
Hangzhou 310027, China

DOI: 10.1002/adtp.201800024

ambient temperatures and easily optimized to achieve optimum conditions for the production of nanoparticles (NPs) applicable to numerous pharmaceutical applications.[4,5]

This review primarily presents the current and future status of DD systems with respect to EHDA, while focusing on several related aspects, including underlying principles, engineering components (related to EHDA), and recent developments in advanced structure fabrication.

2. Electrohydrodynamic Atomization

2.1. Key EHDA Components

The basic setup of EHDA consists of five key components: syringe (hosting medium or formulation which is typically an active-containing formulation), syringe infusion pump, conductive needle (processing outlet for media), high-voltage supply (typically up to ≈30 kV), and a plate ground electrode functioning as a collection plate.

2.2. Main EHDA Engineering Processes

EHDA is a process by which electrical forces are employed to atomize liquids. Liquid or formulation is infused from a syringe into a conducting needle where an electrical field is applied. Solvent evaporation occurs as the liquid exits the nozzle, forming particles or fibers.[6] The resulting structures are then retrieved on a collection plate positioned under the nozzle, usually 10–20 cm below the tip. Several factors have an influence on the products: process parameters (flow rate [FR], applied voltage [AV], collection distance), and liquid physical properties (surface tension [ST], electrical conductivity [EC], viscosity).[7] Subsequently, EHDA has two main well-recognized forms of processing: electrospraying (particle production) and electrospinning (fiber production). Based on these two categories, various EHDA systems have been developed, yielding an

2.2.1. Electrospraying

Electrospraying (Esy) is a cost-effective, one-step process used for the fabrication of micro- and nanoparticles. The very first concept of electrostatic phenomena was observed by William Gilbert in the late sixteenth century.[8] Here, it was observed that a droplet of water deformed into a cone in the presence of charged amber. More than 200 years later, the concept of using electrostatic forces to atomize liquids was proposed by Lord Rayleigh. Rayleigh hypothetically predicted that a liquid droplet would become unstable when reaching a threshold charge, a threshold confirmed a century later, now known as Rayleigh's limit.[9,10] He found that the droplet would break down into finer droplets via coulombic fission. Zeleny exploited this theory to demonstrate how electrostatics affects the behavior of liquids, using capillary-plate configuration, a similar setup used in the present day.[11] His work involved experimental research which provided evidence for several Esy modes including dripping, pulsating, and cone jet.[12]

Muhammad Sohail Arshad is an associate professor at the Bahauddin Zakariya University, Pakistan. He obtained his bachelor and masters degrees from the University of the Punjab and subsequently pursued a Ph.D. at The Leicester School of Pharmacy, UK. He is an expert in pharmaceutical technologies and formulation science. His research highlights include transdermal drug delivery, (microneedle- and patch-based drug-delivery systems), 3D printing of biomaterials, and site-specific drug-delivery approaches. He has also established expertise in EHDA-related methods and spray-drying and freeze-drying technologies.

Ming-Wei Chang is an associate professor at the College of Biomedical Engineering and Instrument Science, Zhejiang University (ZJU), China. He was appointed at ZJU in 2013, following his position as an associate researcher at the Institute of Biomedical Engineering (University of Oxford). He obtained his Ph.D. in biomedical engineering from the University College London and has served as an R&D manager and principal investigator for 5 years at the Industrial Technology Research Institute (ITRI, Taiwan). He has a keen interest in smart and new materials (from flexible materials to designer 3D and 2D products) and methodologies to engineer micro/nanostructures (including EHDA, gyration/centrifugal, printing, ultrasound, and advanced combinatorial processes) for biomedical applications and healthcare technologies.

Zeeshan Ahmad is a professor of pharmaceutics and drug delivery at the De Montfort University (The Leicester School of Pharmacy), UK. He obtained his bachelor and doctoral degrees from Queen Mary (University of London) and has held several research posts and fellowships (from EPSRC, the Leverhulme Trust, and the Royal Society). He also leads the EPSRC EHDA Network (a highly interdisciplinary initiative involving several pharma industries and academia). He has broad research interests in medical materials, their engineering (EHDA, microfluidic, printing, centrifugal/gyratory, and numerous established pharmaceutical processes), and applications toward improving healthcare (interfacing at chemistry, biology, physics, and engineering).

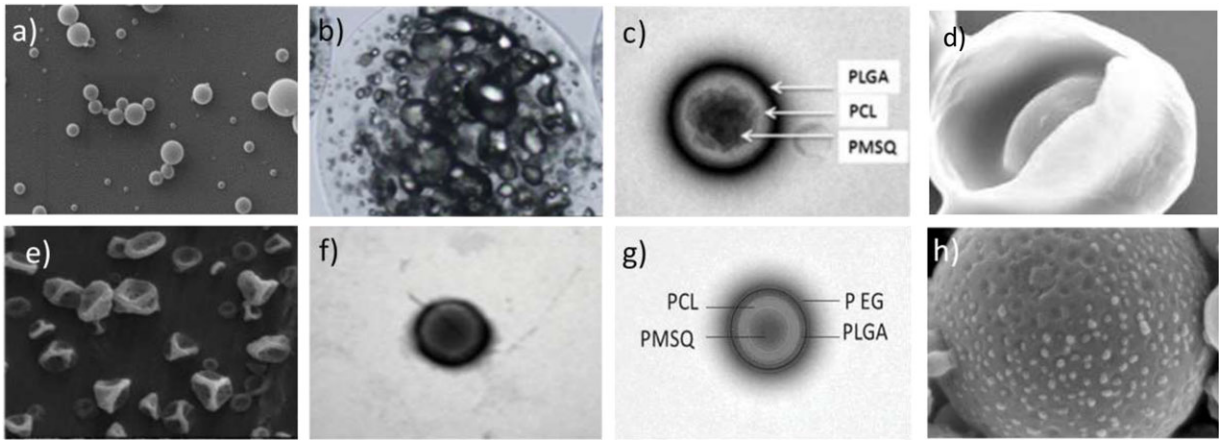

Figure 1. Examples of EHDA particle systems showing a) SEM image at ×50 k of electrosprayed PVP particles loaded with timolol maleate using single-needle setup; reproduced with permission.[14] Copyright 2017, Elsevier. b) TEM image showing multi-core alginate capsules containing epoxy resin engineered using single-needle electrospraying system to develop novel self-healing containers; reproduced with permission.[92] Copyright 2016, Nature. c) Bright-field TEM image of trilayered particles (PMSQ core, PCL intermediate, and PLGA shell) produced using a novel triple-needle EHD device; reproduced with permission.[231] Copyright 2013, Elsevier. d) Egg-yolk-like structures using tri-needle coaxial engineering; reproduced with permission.[234] Copyright 2017, ACS. e) SEM image at low magnification of porous ERS/PMMA core/shell nanoparticles using 4% PMMA; reproduced with permission.[117] Copyright 2015, Elsevier. f) TEM image of electrosprayed nanoparticles made of PVP and PLGA. Reproduced with permission.[118] Copyright 2014, Elsevier. g) Bright-field TEM image demonstrating the engineering of particles with four distinct layers: an inner core of PMSQ, inner intermediate layer of PCL, outer immediate layer of PLGA, and an outer shell of PEG. Reproduced with permission.[232] Copyright 2014, Wiley. h) High-magnification SEM images of strawberry-like SiO_2 microspheres loaded with silver nanoparticles; reproduced with permission.[287] Copyright 2011, IOP.

In the 1960s, Taylor experimented with the balance between ST of liquids and electrical forces, which later developed the underlying theory of Esy.[10] He found that there was a threshold where the electrical field was in equilibrium with the ST of the liquid, which resulted in a stable jet.[10] This characteristic jet is known as the Taylor cone, now a prerequisite for the production of small, spherical structures.

Esy has already proven its potential in an array of applications (**Figure 1**), including protein delivery, gene therapeutics, and antibiotic delivery. However, there are still many arenas in which this method can be further exploited, for example, transdermal administration[13] and ocular drug delivery.[14]

2.2.2. Electrospinning

Electrospinning (ES) is a versatile, simple, cost-effective method capable of producing polymeric micro- and nanoscaled fibers. The theory of producing 1D structures using ES was proposed over a century ago by Morton,[15] whose work was influenced by Rayleigh's observations made in 1897.[16] Extensive research was carried out by very few scientists, the most notable work was carried out by Zeleny.[11] Many systems have since been patented;[15,17–19] one of the earliest patent filed by Anton Formhals in 1934 demonstrated the use of electrodes to focus the cone jet to a rotating cylinder. The interest in the ES process spiked in the 1980s in tune with the interest in nanotechnology. This is reflected in the number of publications that were circulated; the number more than tripled in the period of 2005–2010. The first concept paper on using the ES process for fabricated 1D fibrous structures was only proposed in the mid-1990s by Doshi and Reneker, where fibers within the range of 0.05–5 μm[20] were produced.

ES allows the production of continuous fibers as a result of the electrical field stretching the infused polymeric solutions at the needle exit. The jet does not break up but elongates to form fibers of nanometer width.[21] Due to the unique morphology of these structures, they can be used in a wide range of applications (**Figure 2**) including bioengineering,[22] ophthalmics,[23] and drug delivery.[24]

2.3. Characterizing the EHDA Jet

Extensive research surrounding EHDA processes has resulted in various jetting modes being established, with a set of definitions of proposed modes as well as process of formation. Characterization of these modes have been evaluated in abundance, in the literature, based on intensity and droplet diameter, both of which are affected by liquid physical properties and EHDA process parameters.

2.3.1. Modes of EHDA

The EHDA mode which presents is determined by how the liquid jet breaks up.[25] There are two modes which have been recognized: dripping mode and jetting mode. In the dripping mode, the liquid breaks up at the capillary exit resulting in particles larger than the capillary diameter. Jetting mode occurs when the liquid breaks up in fragments some distance from the capillary exit, causing a continuous jet. Various subcategories have been established, broken down (**Figure 3**a–f). The most

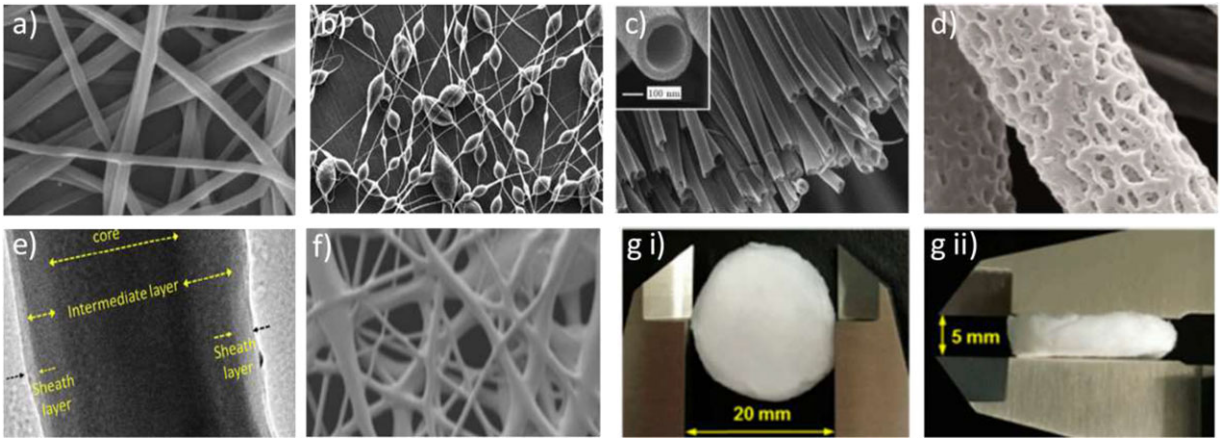

Figure 2. Examples of EHDA fibrous systems showing a) SEM image demonstrating the production of simplistic polymer–drug (PVA–timolol maleate) nanofibers using a single-needle electrospinning system; Reproduced with permission.[167] Copyright 2014, Elsevier. b) SEM micrograph of electrospun PBS-beaded fibers when using dichloromethane as a solvent; Reproduced with permission.[42] Copyright 2008, Wiley. c) SEM image of hollow nanofibers consisting of TiO_2 and PVP shell using a coaxial spinneret; reproduced with permission.[173] Copyright 2012, Scientia Iranica. d) SEM images highlighting the engineering of porous PLA/PEO fibers; reproduced with permission.[288] Copyright 2017, Wiley. e) TEM image demonstrating the novel application of triaxial electrospinning by engineering trilayered fibers with a PVP/nisin core, PCL intermediate layer, and a cellulose acetate shell; figure taken from reference.[239] Copyright 2017, Elsevier. f) SEM image of an example of fibers hosting inorganic material (layered double hydroxide nanoparticles) which acted as drug carriers for enhanced drug delivery Reproduced with permission.[289] Copyright 2017, RSC. g) Fabrication of 3D fibrous scaffolds using PLGA: i) showing a scaffold diameter of 20 mm and ii) a thickness of 5 mm. Reproduced with permission.[179] Copyright 2016, MDPI.

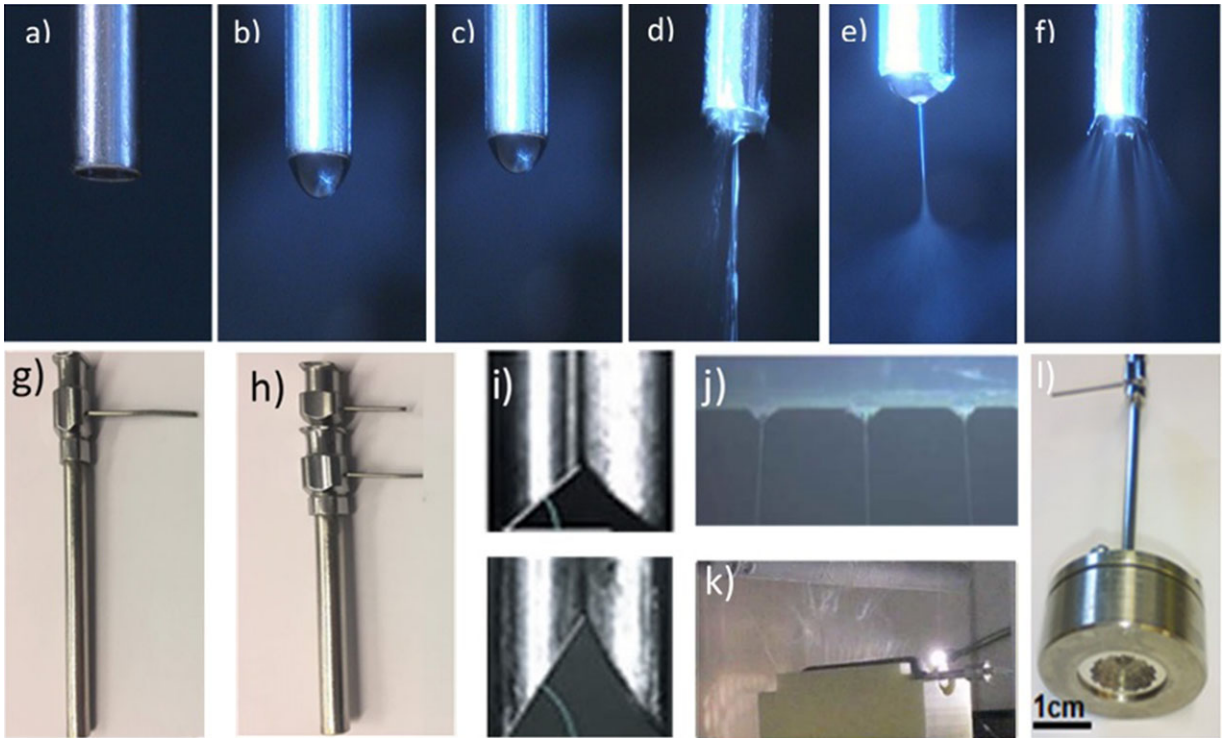

Figure 3. Jetting and nozzle designs. Showing digital images near the needle exit: a) No medium flow, b) infusion of medium with no voltage, c) microdripping, d) unstable jetting, e) stable jetting (cone jet), f) multijet modes. Various types of EHDA needles showing g) digital images of a standard single stainless steel needle and h) coaxially arranged concentric needles. i) Digital image of angular stainless steel needles with the top image showing $\theta = 30°$ and bottom image showing $\theta = 60°$. Reproduced with permission.[281] Copyright 2016, RSC Advances. j) Digital image of three stable jets forming using a horizontal flute-type multipore electrospraying device; Reproduced with permission.[258] Copyright 2015, RSC. Advances. k) Digital image of needleless approach to electrospinning PAN fibers using coil wires to generate stable, dense jets; Reproduced with permission.[286] Copyright 2016, RSC Advances. l) Multi-needle-tip stabilizing emitters. Reproduced with permission.[264] Copyright 2018, Springer.

stable mode is the cone jet, dependent on physical parameters of the liquid as well the liquid infusion rate and the voltage applied to the system.[26] This mode results in spherical, near-uniform, miniaturized particles. The production of fibers is a result of instabilities experienced by the jet causing the solution to "stretch" at the nozzle exit.[21] Non-axisymmetric instability of the cone-shaped jet causes it to invert, resulting in a single rapidly bending strand.[27,28] The resultant fibers have been found to reach several meters in length with nanoscale widths.[29]

2.3.2. EHDA Parameters and Attributes

Media or formulation selection should focus on viscosity, EC, and ST. These parameters significantly affect the jetting stability and the outcome of the EHDA process.[30–32]

Physical Properties of the Solution: Characterization of solutions is important as this will determine the properties of the resulting products.[33] As an electrical field is applied in order to "atomize" the liquid, it is vital the liquid is conductive.[34] Materials with low EC, such as heptane (EC = 0.3 pS m^{-1}), would not be able to produce a stable jet. Liquids with EC lower than 10^{-10} S m^{-1} would not be able to carry sufficient charge, leading to an unstable jet and, therefore, yield polydisperse particles.[35] The viscosity of the infused solution will determine whether Esy or ES will occur.[36,37] Husain et al. demonstrated that the transition between particles and fibers is predominantly reliant on polymer concentration, and in turn viscosity.[37] Low-viscosity liquids present a stable cone jet, yielding small, near-uniform particles while high-viscosity liquids (high polymer concentration) encourage jet stretching at nozzle exit, hence producing fibers.[36,38] ST is an important parameter to consider in EHDA, as liquid breakup is a result of electrical forces overcoming the ST of liquid. Liquids with ST over 50 mN m^{-1} would not produce a stable jet, as the electrical field would be exceeded when voltage is applied. Therefore, solvents of low ST such as ethanol, methanol, and dimethyl sulfoxide (DMSO) are commonly used in EHDA.

Processing Parameters of EHDA: Both AV and FR are used to control the jetting mode and therefore affect the particle size (PS).[39] Altering the voltage can result in various jetting modes.[40] Some literature has suggested that increasing the voltage has found to yield structures with large diameters, while some research groups have found the opposite.[41] This shows that voltage can influence product diameter and must be optimized for specific formulations. The rate at which the liquid is infused through the system can also significantly affect PS. The FR must be slow enough for the solvent to evaporate so that spherical particles are generated. Too high an FR and beaded fibers will form due to restricted time for the solvent to fully evaporate before reaching the collection plate.[42] The working distance (WD) between the capillary exit and the collector must also be optimized or altered for each polymeric solution given that it affects the electrical field strength.[43] If the WD is too short, the solvent is unable to evaporate quickly enough. However, if the WD is too large, beaded fibers can be generated.

Scaling Laws: Universal scaling laws for EHDA processing have been widely applied to investigations surrounding the disintegration of liquid droplets upon application of an electric field. The reciprocal relationship between process parameters and liquid properties can affect the formation and stability of the Taylor cone jet. These variables in turn can affect droplet diameter and current intensity. As a result of this, it is critical to quantify and scale these variables. Gañan et al. have devoted many papers to establish and validate scaling laws.[44–52]

Gañan found that the total emitted current and stable jet diameter can be calculated as a function of physical liquid properties.[45] Based on the vast range of physical properties that materials and solvents possess, the minimum flow rate of the solution can be calculated. Barrero and Loscertales found that the minimum flow rate for highly conductive liquids with low viscosity can be scaled as

$$Q_{\min} \approx \frac{\varepsilon_r \gamma}{\rho K} \tag{1}$$

where $Q_{\min}$ is the minimum flow rate, γ is the surface tension of the liquid, ρ is the density of the liquid, K is the conductivity of the liquid, and ε_r is the permittivity of the liquid. However, with the evolution of the EHDA process, scaling laws also advanced. Equation (1) did not take into consideration the nozzle diameter; hence, the scaling laws were modified to account for this (Equation (2)).

$$Q_{\min} \approx \frac{\gamma D^2}{\mu} \tag{2}$$

where D is the nozzle diameter and μ is the liquid viscosity.

Advantages and Limitations of EHDA: Compared to conventional production/encapsulation techniques, EHDA is undervalued. It is a simple process which is easily operable and amendable. Unlike more orthodox methods, EHDA yields structures which possess high encapsulation and/or loading efficiencies while achieving narrow size distribution. The low operating costs and the little residue that it generated makes EHDA an attractive particle production method. Methods such as spray drying and freeze drying use harsh processing conditions (i.e., temperature) to produce particles. These conditions can severely affect the materials being processed. High temperatures can cause denaturation of sensitive materials such as biomacromolecules like proteins and peptides. The atomization of materials here uses evaporation of solvent to produce dry particles without damaging the polymer or therapeutic actives. While denaturation via temperature can be avoided, some degradation can be initiated by the shear stress in the needle through which the liquid is infused.[53,54]

3. Applications of EHDA

EHD spraying has been developed and utilized in an array of applications including the delivery of different therapeutics such as proteins and antibiotics in nano- and micro-meter-size encapsulated architectures, delivery of hydrophilic and hydrophobic drugs with enhanced loading efficiencies, the production of ultrathin films as well as production of fibrous and porous structures.

Table 1. Selected applications of single-needle electrohydrodynamic atomization.

EHD process	Carrier	Active	Purpose	Size [nm]	Reference
	Mesoporous silica	Kaz-3	Loading of cancer therapeutics	<2000	[72]
Electrospraying	N/A	Insulin	Diabetes mellitus	98–117	[57]
	PEG	Montmorillonite clay	Controls diffusive properties	As small as 3.7	[90]
	PLGA	Streptokinase	Treatment of thrombosis	37	[59]
	Alginate	Adenovirus	Transduction of cancer cells	<150 000	[66]
	Acetylated inulin	Indomethacin	Anti-inflammatory	3000	[79]
	Polyethyleneimine	Plasmid DNA	Delivery to pulmonary epithelium	N/A	65PNIPAM
	PVP/PNIPAM	Timolol maleate	Glaucoma	<200	[14]
	N-octyl-*O*-sulfate	Angiotensin II	Peptide delivery	105.7 ± 4	[63]
Electrospinning	PVA/PCL	Timolol maleate, dorzolamide hydrochloride	Glaucoma	200–400	[167]
	PLA/PLGA	Cisplatin	Cancer therapy	500–1700	[145]
	Chitosan	Hydroxyapatite	Bone generation	277 ± 154	[22]
	PEO	Isolated stretched DNA	Gene therapy	100–350	[139]
	PLAGA	Cefazolin	Antibiotic delivery	470–490	[150]
	Chitosan, polyurethane	Silver sulfadiazine	Wound dressing	N/A	[162]
	PVP	Borneol	Encapsulation of volatile material	440 ± 140	[168]
	PLGA	BSA, myoglobin	Protein scaffolds	468 ± 139	[134]
	Polystyrene	Poly(allylamine hydrogen chloride) dextran sulfate sodium	Entrapment of HIV	4.1	[169]

BSA, bovine serum albumin; PCL, polycaprolactone; PEG, polyethylene glycol; PEO, polyethylene oxide; PLA, polylactic acid; PLAGA, poly(lactic-*co*-glycolide); PLGA, poly(lactic-*co*-glycolic) acid; PNIPAM, poly(*n*-isopropylacrylamide); PVA, polyvinyl alcohol; PVP, polyvinyl pyrrolidone.

3.1. Single-Needle Electrospraying

The simplest device configuration of Esy consists of one conducting needle. In this system, the solution or formulation passes through a single needle and once voltage is applied (and optimized), a stable Taylor cone forms at the tip, producing near-uniform particles with distinct shapes. The active pharmaceutical ingredient (API) is incorporated into a polymer–solvent solution, and upon solvent evaporation, the API is uniformly distributed within the polymer matrix. This even dispersion of API also acts as a way of improving the amorphous nature of crystalline drugs, enhancing bioavailability. Other additives may also be included to optimize formulations for specific or targeted applications. As mentioned before, an array of materials have been successfully encapsulated and processed via single-needle electrospraying (SNESy), yielding promising results for various applications,[55] some of which have been summarized in **Table 1**.

3.1.1. Proteins, Peptides, and Amino Acid Delivery

The physical and chemical lability of biomacromolecules (e.g., proteins, peptides) can influence the preparation of such therapeutics. The structure of proteins consists of weak interactions (electrostatic, hydrogen bonding), which can easily be damaged by increased physical and chemical stimuli or various processing conditions of conventional methods where temperature or stress is amplified. Crucial functionalities of the biomaterial become compromised, usually arising from denaturation.[56] Esy is a process that does not require elevated temperatures, allowing protein or thermosensitive material to be encapsulated within a polymeric matrix in a simple one-step process. One of the earliest demonstrations of this was the encapsulation of biologically active insulin.[57] The resulting electrosprayed NPs ranged in diameter (98–117 nm) and were near monodispersed. By decreasing the insulin concentration in the solvent solution (ethanol:water) or the FR, smaller particles were generated.

N-acetylcysteine (NAC), an amino acid, is an active molecule used in several medical conditions or emergencies such as acetaminophen overdose, chest pain treatment in unstable angina, bile duct blockage in infants, Alzheimer's disease, etc. Despite this wide range of uses, NAC has poor oral bioavailability, <10%. In an attempt to circumvent this, Zarchi et al. have successfully produced near monodispersed NAC-loaded poly(lactic-*co*-glycolic acid) (PLGA) NP (116–692 nm) using SNEsy.[58] Once the process parameters were optimized, spherical and smooth particles as small as 122 nm in diameter with encapsulation efficiency (EE) of 54.5% were generated. The in vitro release study of these particles showed a biphasic release profile of NAC from active-loaded NPs. The release was characterized by first initial burst release (dissolution of NAC at the surface of NPs) followed by slower sustained release phase.

PLGA has more recently been used for one of the first investigations involving Esy enzymes. PLGA nanoparticles served as carriers for streptokinase, a vital enzyme in thrombosis which acts to dissolve blood clots in blood vessels.[59] In this study, SNEsy was utilized to encapsulate the enzyme into a PLGA matrix, producing NPs with a mean diameter of 37 nm. While these NPs exhibited high encapsulation efficiency (≈90%), the activity of enzyme was recorded to be 12%. This reduction in activity was most likely an attribute of the <20% enzyme release

from the polymeric matrix within the first 30 min, resulting in more than 80% not being in the presence of the substrate. As a result, inaccurate measurements may be taken.

PLGA has also recently been used to produce microspheres loaded with lysozyme, between 3.76 and 3.89 μm in diameter.[60] These spheres expressed sustained release (80.7%) for 30 days. While the bioactivity of lysozyme was retained during EHDA processing, the time of degradation was reduced, enabling the lysozyme to be active for longer.

Sericin, a product often discarded during silk processing, has been electrosprayed to produce sericin-loaded DMSO nanopowder. Hazeri et al. found that the Esy process produced particles (25 nm) much smaller than other conventional techniques, while the humidity absorption ability of the powder was found to be six times higher than that of the sericin sponge.[61]

Model protein bovine serum albumin (BSA) has also been electrosprayed with low- and high-viscosity alginate-generated particles with mean diameters 1556 ± 51 and 937 ± 158 nm, respectively.[62] The use of the Esy method here overcame the issue of denaturation that biomacromolecules like BSA experience in harsh environments but also improved the oral delivery of the protein. In another study, *N*-octyl-*O*-sulfate chitosan was used to encapsulate peptide angiotensin II, which demonstrated a triphasic release profile with EE of 92 ± 1.8% and average diameter of 105.7 ± 4 nm.[63]

3.1.2. Gene Therapy

The delivery of DNA-based formulations or genes as a pharmaceutical dosage form has undergone difficulties, mainly stemming from instability issues, most commonly loss of DNA molecular integrity. Both formulation and handling of DNA-based preparations require great attention due to the sensitivity of the material. Esy is a promising way of handling and processing sensitive material without the integrity of the materials being compromised. Zeles-Hahn et al. demonstrated this using epithelial cells in the pulmonary system. Stable plasmid DNA/polyethyleneimine aerosols were sprayed using a single needle with the absence of structural alteration of the DNA. The electrical field found to cause mild toxicity reverted to its normal conditions within a few hours of application to the tissue. In vivo results together with these results yield promising outcomes for administering DNA-based therapy to the pulmonary epithelium and various other tissues.[64]

Gene delivery to microorganisms has also benefitted from single-needle EHD technology. PET30a-GFP plasmid DNA was sprayed with gold NPs into noncompetent *Escherichia coli* cells.[65] Incorporation of gold NPs greatly enhanced the transformation efficiency (five- to sevenfold) compared to sprayed naked plasmids. In addition, the preparation and time required to develop these products using conventional methods were eliminated in the Esy process.

Park et al. utilized Esy to entrap adenovirus (Ad). In an attempt to protect and achieve sustained release of Ad, cross-linked alginate beads were fabricated.[66] Process variables (AV, alginate concentration, FR) were all found to have a significant effect on the size and morphology of the alginate beads. An alginate concentration of 0.5% w/w produced beads with high encapsulation activity and sustained release for 7 days. Alginate beads smaller than 150 μm were developed using concentrations of <1% and flow rates <2.5 mL h^{-1}, as a result of low viscosity of the Ag solution. In addition to this, the beads were used for the transduction of U343 glioma cells. The Ad released from the beads had high transduction efficiency in cancer cells, highlighting the potential of Esy beads to overcome the limitation of liver accumulation and immune response.

3.1.3. Cancer Therapy

Regardless of numerous chemotherapy drugs available for treatment, both orally and intravenously, the treatment is still met with copious limitations. Physical properties such as drug solubility and poor pharmacodynamics of the drug at physiological conditions can lead to ineffective treatment. Using Esy to load anticancer drugs into polymeric structures, a much higher dose can be delivered directly to the tumor, overcoming the need for repetitive drug administration.

Anticancer drug hydroxycamptothecin was encapsulated in poly(benzyldehyde-polyethylene glycol) poly(D,L-lactide) (PGBELA) NPs, achieving an encapsulation efficiency of 80%. In vivo testing with Hepa2 cells and H22 tumor–bearing mice showed a reduction in side effects, such as tissue necrosis and tumor growth, compared to existing methods.[67] Doxorubicin (DOX) and tamoxifen are common drugs used in the treatment of breast cancer and have been electrosprayed to produce NPs. Wu et al. incorporated DOX into elastin-like polypeptides (ELPs) to produce biodegradable and biocompatible NPs ranging from 300 to 400 nm in diameter,[68] while Cavalli et al. loaded tamoxifen into poly(amidoamine)-cholesterol NPs (500 nm) in a powder form in a single one-step process.[69]

Anticancer drug cyclophosphamide is often combined with DNA to treat cancers such as retinoblastoma, neuroblastoma, and breast cancer. It is thought that the mechanism of action involves the disruption of DNA replication of cancer cells. Gulfam et al. successfully controlled the release of cyclophosphamide using natural gliadin polymer as a carrier.[70] Using 7% gliadin polymer, a drug-loading efficiency of 72.02 ± 5.6% was achieved in homogenous particles with an average diameter of 218.66 ± 5.1 nm. Gradual drug release from the gliadin NPs was observed over a 48-h period, while in vivo analysis exhibited downregulation of BCL-2 protein in breast cancer cells upon exposure to cyclophosphamide-loaded particles for 24 h.

More recently, hyaluronic acid derivative nanocomposites were developed as carriers for resveratrol, for local tumor treatment.[71] The amphiphilic nature of hyaluronic–ceramide combined with solubility enhancer, Soluplus, enabled more than 80% of the drug to be entrapped within the nanocomposites. This combination of materials demonstrated higher cellular uptake efficiency in CD44 receptor and positive human breast cancer cells compared to Soluplus nanocomposites alone. The nanocomposites (230 nm) demonstrated sustained, pH-dependent release while showing decrease in in vivo clearance, highlighting the potential in theranostic nanosystems for receptor-expressed cancers.

Using SNEsy, APIs can be encapsulated and dried simultaneously within the pores of inorganic materials, demonstrating improved pharmaceutical manufacture properties compared to conventional processes, for example, solvent evaporation.[72]

3.1.4. Nonsteroidal Anti-Inflammatory Drugs

Nonsteroidal anti-inflammatory drugs (NSAIDs) are APIs associated with pain mitigation and reduction of inflammation. They work by interfering with cyclooxygenase, an enzyme which controls the production of prostaglandins. Oral administration through tablets is the most common route to deliver NSAIDs. Esy can bypass the laborious manufacture of tablets and develop NSAID-loaded structures on demand with increased drug loading, eliminating the need for frequent dosage.

Bohr et al. developed PLGA microspheres loaded with celecoxib using a single conductive needle.[73] Celecoxib is an insoluble (orally) COX-2 selective NSAID which targets cyclooxygenase-2 (responsible for pain and inflammation). These biodegradable structures ranged between 2 and 8 μm, with encapsulation efficiency of 88–99%, which is considerably higher than existing encapsulation methods such as emulsification.[74,75] The drug remained in its amorphous state and remained stable for up to 8 months. Compared to spray drying, Esy of celecoxib provided much more control of drug release as well as improved control of particle characteristics (size, morphology).[76] This outcome proves that Esy can provide a basis for successful oral delivery of practically insoluble drugs, leading to increased bioavailability (BA) of such drugs.

Piroxicam, an analgesic NSAID, is described as a class 2 drug in the Biopharmaceutical Classification System— low aqueous solubility and high permeability. A Finnish research group yielded an unknown polymeric form of piroxicam when a solution of piroxicam dissolved in chloroform was electrosprayed.[77] Three polymorphs (I, II, III) have currently been established, with Esy now presenting a fourth. X-Ray diffraction (XRD) and Fourier transform infrared (FTIR) spectra demonstrated an unknown crystal structure with evident changes when compared to the spectra of piroxicam I; new functional groups and chemical bonds were present in Esy particles (11.4 μm). Scanning electron microscopy (SEM), differential scanning calorimetry (DSC), and high pressure liquid chromatography (HPLC) found that the sprayed particles were spherical in shape and showed no signs of degradation during 127 days of storage. Piroxicam has also been loaded into polyvinylpyrrolidone (PVP) nanospheres which exhibited 15-fold higher release rate and threefold higher AUC when compared to piroxicam powder.[78] This enhanced oral BA shows that Esy can help improve the release and delivery of poorly water-soluble drugs.

Indomethacin, a multiple use NSAID, was successfully loaded into acetylated inulin (a naturally occurring polysaccharide) particles (3 μm) using chloroform as a solvent.[79] Indomethacin, 10% w/w, was added to an inulin–chloroform mixture, and with optimized processing parameters, spherical microparticles were produced (EE = 35.39 ± 1.63%). The drug remained in its amorphous state, confirming the reproducibility of the EHDA process. The acetylation of inulin in this study shows Esy to be an advantageous approach to generate particles with specific characteristics while not disrupting the colon-targeting ability of actives such as inulin.

Liposomes, amphiphilic phospholipid systems, are capable of encapsulating both hydrophilic and lipophilic drugs with high drug loadings (as a result of high thermodynamic stability).[80] They have been utilized in an array of applications including vaccines,[81] cancer therapy,[82] ocular drug delivery,[83] and the delivery of NSAIDs. Naproxen- and lecithin-loaded PVP microparticles have been prepared using Esy as templates for molecular self-assembly for in situ liposome synthesis.[84] The liposomes, self-assembled from Esy composites, demonstrated high EE (91.3%), and in vitro release analysis showed 80.7% drug release over 24 h via Fickian diffusion.

3.1.5. Miscellaneous

Prabhakaran et al. from Singapore demonstrated the production of biocompatible PLGA microspheres using SNESy. Solvents dichloromethane (DCM) and trifluoroethanol (TFE) were used to help encapsulate antibiotic metronidazole (MDZ) in a PLGA matrix, yielding spheres 3946 ± 407 and 1774 ± 167 nm in diameter, respectively. The spheres exhibited release for at least 41 days via Fickian diffusion, demonstrating a potential substrate for periodontal regeneration.[85]

PLGA has also been used to encapsulate simvastatin, an HMG CoA reductase inhibitor.[86] The electrosprayed simvastatin-loaded PLGA particles achieved high EE (90.3%) while exhibiting sustained release of the statin. Optimization of the EHD process yielded particles with average diameter of 166 nm with enhanced aqueous stability, highlighting the appreciable biocompatibility of the PLGA carrier.

More recently, the evolution of pharmaceutical applications has yielded more complex drug-delivery devices and dosage forms. Mehta et al. were the first to utilize SNEsy for novel engineering of on-demand coated contact lenses.[87] These rapidly dissolving probe-loaded PVP particle coatings demonstrated high loading efficiency, and with uniform particle size distribution, PVP particles less than 100 nm in diameter were observed. Mehta et al. have also developed PVP/poly(*N*-isopropylacrylamide) (PNIPAM) matrix loaded with even distribution of antiglaucoma drug timolol maleate.[14] These structures were used as coatings on commercialized contact lenses, with more than 52% of the nanostructured coatings being less than 200 nm in diameter. The coatings demonstrated a biphasic release profile, an initial burst release of drug followed by a sustained release via quasi-Fickian diffusion. These preliminary studies suggest that the on-demand EHD processing of such materials for the novel application in ocular drug delivery has great potential, which is yet to be further explored.

More recently, a research group in USA utilized SNESy to fabricate cell-laden polyethylene glycol (PEG) microspheres.[88] These spheres had controlled diameters (70–300 μm) with high cell encapsulation efficiency (>90%). Prompting cell–matrix interactions (via peptide modification) led to uniform cell dispersions throughout the polymeric matrix. Qayyum et al. found that by using increased voltage (>5 kV), cell distribution

within the PEG spheres was disturbed. The fabrication of such hydrogel microspheres using Esy can be greatly exploited by an array of biological applications including injectable cell delivery.

SNESy has not only been used to entrap actives or materials, as previously discussed, but also to modify polymeric matrices of particles. Montmorillonite (MMT) clay is an aluminosilicate often incorporated into polymeric formulations to modify diffusion properties of delayed release materials.[89] The encapsulation of MMT clay (3%) within the PEG matrix with Esy improved the mechanical properties of the nanobeads produced, benefitting the interactions between the beads and the surrounding tissues.[90] The diameters of the PEG beads ranged between 90 and 150 nm, with increased amounts of clay within the beads producing smaller beads (3.7 nm).

Stimuli-responsive systems used in conjunction with EHDA have great potential in biomedical engineering. Hayashi et al. utilized SNEsy to atomize magnetic materials (iron-organic compound) for dual-imaging modality.[91] Red-cell-like magnetic particles (loaded with fluorescent dye) were yielded, which could be used as fluorescent markers as well as in magnetic resonance imaging.

The use of SNESy often results in the production of particles with even molecular distribution of active within a matrix. However, Hia et al. utilized a single needle to electrospray an epoxy resin–alginate solution which resulted in the fabrication of core/shell particles (320 ± 20 μm), structures usually seen with coaxially arranged conductive needles.[92] As a result of this multilayered structure, the particles had the ability to heal up to three times more than single-compartmented particles.

3.2. Coaxial Electrospraying

SNEsy is the most simple device setup. Developments in EHD devices led to the assembly of the coaxial system. Here, two conductive needles are used in conjunction, in a coaxial arrangement. This configuration is valuable in the one-step encapsulation of APIs and therapeutics within a polymeric shell. It is crucial that the materials used in each needle are immiscible, allowing the coaxially aligned needles to produce particles within a defined shell (polymer) and defined core (API). The alignment of the inner needle can either protrude the outer needle or sit inside the outer needle.[93] The polymeric shell often has dual function, prolonging the release of the active and providing protection to the active from harsh, external environments, such as acidic conditions in the stomach.

The use of polymers as carriers/vehicles to encapsulate APIs has gained a great deal of interest in the pharmaceutical research arena in recent years. Loading APIs and therapeutic agents within polymeric carriers can support controlled drug release, providing a constant therapeutic concentration at the targeting site. Existing methods to produce structures such as emulsification and solvent evaporation have been met with limitations such as API denaturation and poor BA. Coaxial Esy (CEsy) evades these disadvantages and is able to produce core/shell structures with complex release kinetics while not compromising the API structure and function. A major advantage of a coaxial device is the ability to produce micro- and nanosized carriers, for example, micro- and nanocapsules with narrow size distributions with accurate targeting abilities.[94–96] **Table 2** highlights some of the developments using coaxial setup in Esy.

3.2.1. Microcapsules

Loscertales et al. were the first to propose the use of two conjunctive needles. Using a coaxial setup, capsules with a water core and olive oil shell, ranging from 150 nm to 10 μm in diameter, were produced.[97] Process optimization allowed Chen et al. to recognize that when utilizing two needles, the outer liquid flow rate determined the properties of the cone jet itself.[98]

The coaxial device was used to fabricate ceramic suspension microparticles encasing a ceramic suspension (10% w/w alumina and glycerol) within a polymethylsilsesquioxane (PMSQ) shell. The polymeric solution was sprayed at an FR (30 μL min^{-1}) twice as fast as the ceramic suspension (15 μL min^{-1}). SEM confirmed the increase in capsule size (from between 2.6 and 3.4 μm to between 1 and 38 μm) from polymer-only particles to microcapsules, respectively, providing sufficient evidence for encapsulation.

Like SNEsy, CEsy has the ability to encapsulate biomacromolecules such as proteins and peptides without denaturation and degradation. Insulin, a peptide produced in the pancreas, is responsible for the regulation of carbohydrate and fat metabolism. It is a hormone that is usually produced by the body. However, if insulin production is compromised, diabetes mellitus (diabetes) can result.[99] CEsy has been combined with ionic gelation to evaluate the capability of the process to produce insulin-loaded microcapsules. Chitosan capsules (232 μm) generated for the potential oral delivery of insulin were generated with sizes considerably smaller than those produced using ionic gelation alone.[100] An EE of 92% was achieved, showing the potential of a much simpler, more effective, and patient-compliant method for the oral delivery of insulin for those who suffer from type 1 diabetes (failure of insulin production). Li et al., a research group from China utilized silk fibroin to develop functionalized dressings loaded with bioactive insulin.[101] The encapsulation of insulin within the inner layer of the particles sustained/delayed release for up to 28 days, with the sponge dressing successfully accelerating chronic wound healing.

Much larger proteins than insulin such as BSA (molecular weight 66.5 kDa) have also been used to produce protein-loaded capsules. CEsy was used to encapsulate BSA along with lysozyme to overcome implications associated with other orthodox methods of protein encapsulation such as denaturation and aggregation. SEM indicated smooth, spherical PLGA particles (3.4 μm), with fluorescence microscopic analysis showing evidence of successful of BSA (a natural fluorophore).[30] The lysozyme retained more than 9% of its bioactivity when released, proving that the structure and function were not compromised by the Esy process, with in vitro release studies showing that the release of the biomacromolecules was sustained for more than 30 days. BSA has also been encapsulated into biodegradable PLGA capsules to assess the ability to deliver proteins which exhibited high EE and particles between 3 and 5.5 μmm.[56]

Table 2. Selected applications of coaxial electrohydrodynamic atomization.

EHD process	Carrier		Active	Purpose	Size [μm]	Reference
	core	Shell				
Electrospraying	Insulin	Chitosan	Insulin	Diabetes mellitus	232	[100]
	BSA, lysozyme	PLGA	BSA, lysozyme	Protein delivery	3.4	[30]
	Alginate	Zein	*Lactobacillus acidophilus*	Microorganism carriers to gastrointestinal tract	312 ± 69	[102]
	PLGA	Chitosan	Artesunate	Cancer therapy	30.393	[109]
	Shikimic acid	PLA	Shikimic acid	Improve oral bioavailability	–	[110]
	PVP/PLGA	PCL/PLGA	Naproxen, rhodamine B	Antibiotic encapsulation	–	[118]
	Eudragit RS	PMMA	Metronidazole	Antibiotic encapsulation	0.06	[117]
Electrospinning	PVA	Chitosan	Doxorubicin	Cancer therapy	0.28	[181]
	PVA	Alginate, PEO	BSA	Colon-specific controlled release	0.455	[194]
	Gentamycin sulfate	PCL	Gentamycin sulfate	Antibiotic encapsulation	0.208–1.585	[184]
	Resveratrol	PCL	Resveratrol	Antioxidant encapsulation	0.153–1.317	[184]
	PCL	PVA/gelatin	Bromelain, salvianolic acid B	Wound healing	0.4–0.5	[178]
	Polyethylene glycol methacrylate	PLLA	N/A	Development of vascular stents	–	[197]
	Zein	PVP	Ketoprofen	NSAID delivery	0.730 ± 0.190	[187]
Microbubbling	Air	Phospholipid		Imaging	<7	[121]
	Air	Glycerol	Air	Imaging	3.0–60	[122]
	Air	2,2'-azobis(isobutyramidine) dihydrochloride polystyrene	Air, BSA	MB production for protein delivery	40–800	[126]
	Air, BSA	Silk fibroin	Air, BSA	Biological scaffolds	240–1000	[127]
	Air	tPA-BSA	BSA	Bubble production for ischemic stroke therapy	41	[128]
	Air	tPA-Phospholipid	Lipid	Bubble production for ischemic stroke therapy	3.0–60	[129]
	Air	tPA-Lipid	Lipid	Ultrasound marker	–	[130]

BSA, bovine serum albumin; NSAID, nonsteroidal anti-inflammatory drug; PCL, polycaprolactone; PEO, poly(ethylene oxide); PLA, poly(lactic acid); PLGA, poly(lactic-*co*-glycolic) acid; PLLA, poly(L-lactic acid); PMMA, polymethyl methacrylate; PVA, polyvinyl alcohol; PVP, polyvinyl pyrrolidone; tPA, tissue plasminogen activator.

A combination of alcoholic acidification and CEsy has been found to produce adequate delivery vehicles for microorganisms. Live organisms such as probiotic bacteria can be administered to improve the balance of natural flora in the gastrointestinal (GI) tract, preventing the effects of harmful pathogens and innervation of the human immune system. These microorganisms are sensitive to the acidic conditions of the GI tract, for which CEsy can provide sufficient protection. *Lactobacillus acidophilus* is a naturally occurring flora present in the GI tract and mouth of humans. It has successfully been encapsulated into alginate-core and zein-shell capsules.[102] An AV of 6 kV yielded capsules with an average diameter of 312 ± 69 μm; when increasing the AV to 10 kV, the average diameter decreased to 259 ± 62 μm. By combining these two novel techniques, the survival of the probiotic was improved fivefold "illustrating potential of alginate–zein core/shell microparticles"[102] for carriers in the GI tract.

Multilayered alginate microcapsules encapsulating *L. acidophilus* were also produced using CEsy.[103] Combining CEsy with fluidized bed coating produced capsules with EE higher than 90%, with a much higher degree of protection to the entrapped probiotic compared to previous studies. Upon exposure to heat, the entrapped cells demonstrated vitality loss of only 0.6 log CFU g^{-1}. This production of heat-resistant microcapsules with a combination of techniques can pave the way for protection of other thermosensitive materials.

The presence of the shell layer in CEsy particles is not always to protect sensitive material; it can also act as a way for preventing burst drug release in acidic conditions. Enteric polymer Eudragit L100 was used to produce core/shell particles for the delivery of darunavir, an antiretroviral drug.[104] Hydroxypropyl methylcellulose (HPMC)–darunavir solution was infused through the inner needle of the coaxial arrangement forming the core with Eudragit L100 forming the shell. High EE (90%) and reduction of 20% of darunavir release in acidic conditions as a result of the enteric shell shows the potential of CEsy for encapsulation of poorly soluble and susceptible solid dispersions. The same research group repeated the same study with darunavir nanocrystals, as opposed to solid dispersion nanoparticles, yielding similar results, high encapsulation efficiency, and 20% reduction of drug release.

Eudragit L100 has also been used to fabricate enteric-coated particles containing antiretroviral drug lopinavir and absorption enhancer ritonavir.[105] MPs with average diameter of 1 μm were produced. Encapsulating both actives together found to significantly improve drug release compared to using each active alone, and due to the presence of ritonavir, the absorbance of lopinavir in the GI tract was improved, resulting in a reduction in the number of doses.

A key characteristic of EHDA is generating particles with almost all types of materials, advantageous for poorly soluble materials. Quercetin (Q) is such a material. It is a poorly soluble, naturally occurring pigment found in plants and food. It has been used in the treatment of diabetes and high blood pressure. Its uses also extends to cancer prevention, increasing athletic performance and endurance, as well as allergy prevention.[106] Three systems (with different drug loadings) with PVP:Q (core) and PVP:sodium (shell) were sprayed at various flow rates.[107] SEM and TEM provided evidence of encapsulation of core material, while thermal and structural analysis showed that all the constituents in the formulation were present in the amorphous form, unaffected by the Esy process. Constructive interactions between the components have the ability to improve the dissolution and permeability of Q, a concept which can extend to other poorly water-soluble drugs for oral drug-delivery systems.

Delivery of anticancer drugs is often met with various challenges including solubility and poor BA. CEsy provides a simple, one-step, on demand process of API encapsulation into polymeric carriers for localized delivery at the tumor tissue. Paclitaxel, a drug used to treat an array of cancers including breast cancer and ovarian cancer, was encapsulated into PLGA microparticles with the aim of achieving sustained release of drug to locally treat C6 glioma.[108] The resulting particles were of various shapes (spherical, doughnuts), and thermal analysis showed paclitaxel to be present in its amorphous or disordered crystalline state. Following optimization of process parameters (8% w/w PLGA; FR, 5 mL h^{-1}), particles with an average diameter 15.2 ± 1.7 μm with EE of 82.3% were obtained. A sustained release for more than 30 days was exhibited, indicating that the bioactivity of the drug was maintained, highlighting the ability to inhibit C6 glioma cells in vivo. PLGA has also served as a carrier alongside chitosan for the encapsulation of anticancer drug artesunate. CEsy was deemed an advantageous method of particle production for this antiproliferative active due to overcoming issues with instability and limited aqueous solubility of the active.[109] Core/shell particles with a mean diameter of 30.393 μm were yielded with entrapment efficiency of 80.5%.

More recently, the potential for CEsy to improve the bioavailability of antibacterial agents was investigated. Using two concentrically aligned needles, shikimic acid was loaded into PLA shells in an attempt to increase the oral BA of shikimic acid by sustaining its release.[110] Shikimic acid is often found in low concentrations in autotrophic organisms, used as a base material in oseltamivir production (Tamiflu). CEsy production of shikimic acid–loaded particles prolonged the period in which the water-soluble active remained in plasma circulation, with improved BA following oral administration. Increased absorption in the intestinal tract (duodenum, ileum, as well as jejunum) was also observed, demonstrating advantages of EHDA in improving clinical applications.

3.2.2. Nanocapsules

Continuous development and optimization of the EHD process has made the concept of producing capsules on a nanoscale a reality.[111]

The polymer PMSQ was employed as a carrier to demonstrate the nanoencapsulation of phase change material perfluorohexane.[112] Chang et al. found through preliminary studies that hollow particles as small as 200 nm could be generated with shell thickness of 30–70 nm. Further research by the same group assessed the ability to control the "thickness of (the) hollow polymeric microspheres."[113] The diameters of the resulting particles ranged between 310 and 1000 nm with shell thickness 40–95 nm. The ability to control shell thickness can be exploited for controlled release of a large array of drugs entrapped in the capsule core.

As previously shown by Xie et al., anticancer therapeutic drugs have been loaded into microcapsules.[108] Subsequently, paclitaxel encapsulation into capsules of nano range (average of 200 nm) has been achieved.[114] Paclitaxel-loaded PLGA capsules were fabricated using organic salts (didodecyldimethylammonium bromide) to increase the conductivity of the spraying solution. An increase in PLGA concentration to above 10% resulted in an increase in particle size. A flow rate of 0.1 mLh^{-1} provided a stable cone jet and yielded monodisperse particles of 200 nm, an adequate size in cancer therapy.

Anticancer drug DOX along with angiostenosis agent Combretastatin A4 were entrapped within the shell and core structures of the NP, producing particles with over 90% EE.[115] Two different polymeric systems were assessed and compared. As a result of enhanced affinity to the incubation media used in the in vitro model, PVP/PLGA NPs exhibited faster and greater drug release compared to poly(ε caprolactone) (PCL)/PLGA NPs, suggesting that sequentially controlled drug release in tumor chemotherapy is a promising application of CEsy.

CEsy has also shown its potential in encapsulating and releasing peptides. Model peptide angiotensin II (a vasoconstrictive peptide hormone) was encapsulated into *N*-octyl-*O*-sulfate chitosan and tristearin nanocapsules (100–300 nm), which exhibited triphasic in vitro release— initial slow release with sequential rapid release, ending with conventional diffusive release phase.[116]

As with SNEsy, CEsy can help enhance drug release as well therapeutic concentration at the targeted site. MDZ is an antibiotic used to treat infections of the mouth and bones and postsurgery infections. Eudragit RS/poly(methyl methacrylate) (PMMA) core/shell particles were loaded with MDZ using a coaxial arrangement.[117] The nanocapsules (60 nm) maintained stable particle size distribution in simulated body fluid (pH 7.4) for 8 h. EE of 100.02 ± 0.92% and 100.37 ± 1.80% were achieved with 2% and 3% PMMA concentrations, respectively.

Naproxen, a hydrophobic antibiotic, along with rhodamine B (hydrophilic) were encapsulated in polymeric NPs with distinct core/shell structures.[118] The one-step process of CEsy yielded particles with 85% EE along with distinct release profiles (maybe as a result of polymer–drug interactions), highlighting the use of this system in the success of combination therapy. The adequate stability and drug controlled drug release characteristics of these NPs demonstrated the potential for clinical application of an

array of APIs, a platform which can be modified for specific targeted drug-delivery systems.

3.2.3. Microbubbling

Microbubbles (MB), microparticles filled with air, have successfully been developed and utilized in a vast array of applications in the pharmaceutical industry, ranging from biomedical uses (diagnostic and therapeutic) to cosmetics. The most common and advantageous use of microbubbles is within the remit of ultrasound imaging.[119] Their ability to scatter and reflect ultrasound waves as well as their high compressibility (a characteristic which enhances scattering ability) makes them more appealing than conventional contrast agents, such as red blood cells. Drugs can be incorporated into the shell or gas core of these bubbles which, when administered, can be traced in the body. Once near the target site, bursts of ultrasound waves stimulate release of the drug. Conventional methods of microbubble production (sonification, microfluid devices) fail to produce monodisperse MB to the extent of Esy, in a fast on-demand one-step process. The first attempt to exploit CEsy for MB production utilized a glycerol–air system which yielded MB with narrow SD, less than 10 μm in diameter.[120]

This insight into the production of microbubbling led to the classification of various modes of electrohydrodynamic flow, (bubble dripping, coning, and microbubbling), all of which are dependent on applied voltage. Farook et al. established that the microbubbling mode was vital for continuous production of MBs. This process was then adapted to produce MB with a phospholipid coating with a mean diameter of 6.6 μm.[121] Along with a high yield of production (10^9 bubbles per min^{-1}), these MBs were found to be stable at room temperature (RT) but decreased rapidly in size at body temperature. After 20 mins, the shape and size of the MBs was maintained at 1–2 μm, highlighting that the elevated physiological temperature increased the diffusion of air through the phospholipid shell.

Parkizkar et al. used EHDA along with a T-junction microfluid device for the preparation of monodispersed MB, using a glycerol–air system. They found that a high viscosity greatly influenced the size of the particles and that on increasing the applied voltage over the threshold of 12 kV, no significant change in the MB size was observed.[122] A simple microfluid device was also used in conjunction with CEsy to produce monodisperse MBs with diameters between 3 and 60 μm.[123]

MB ultrasound contrast agents have also been generated using Esy principles to help improve the efficacy of MB as drug or gene carriers.[124] By combining PEG 400 with glycerol, the MB produced were found to be radically smaller (as small as 4 μm) and had a much longer lifetime when compared to solely glycerol-shell MBs. This indicates a greatly stabilized delivery system for clinical use.

More recent advances in using CEsy for MB production sees multiple-layered lipid MBs being produced with encapsulated silver nanoparticles and perfluorocarbon. Li et al. observed core/shell morphologies with nanoparticles inside the shell.[125] When introduced to broadband light, there was a noted elevation in the temperature in silver nanoparticles suspended in perfluorocarbon, highlighting the potential for a light-triggered drug-delivery system. There has also been an attempt to produce BSA-containing MBs. Mahalingham et al. successfully produced 2,2′-azobis(isobutyramidine) dihydrochloride-polystyrene MBs ranging between 40 and 800 μm, highlighting the potential for production of MBs for the delivery of proteins and peptides.[126] Silk fibroin MBs for biocoatings and tissue engineering have also been fabricated. The hollow pores that the MBs exhibited can be advantageous for various drug-delivery applications.[127] Ekemen et al. also successfully produced BSA-laden MBs and porous films for various drug-delivery systems, scaffolds, and ultrasound contrast agents.[128]

More recently, a research team from Singapore produced stable MBs containing tissue plasminogen activator (tPA) in shell layer (phospholipid or BSA).[129] tPA-BSA MBs were (on average) 41 μm in diameter while 41% of the tPA-lipid bubbles were between 3 and 6 μm. Bubble aggregation usually seen in bubble production was greatly released here. The flexibility of the CEsy process shows great potential for drug-loaded MBs in ischemic stroke therapy. Yan et al. also developed ultrasound-responsive tPA-lipid MBs which disintegrated within a very short period of time (less than 5 min), advantageous for the limited exposure level requirements in the human brain.[130] While high-intensity ultrasound (power of 82%) successfully triggered release of tPA from lipid structures, the MBs also had high encapsulation efficiency, almost 96%.

3.3. Single-Needle Electrospinning

As mentioned before, the viscosity of the liquid being atomized determines whether particles or fibers will form when exposed to the electrical field. The device configuration is exactly as with Esy. A conductive needle is connected to an infusion pump and a voltage supply. However, the liquid displays different behaviors at the nozzle exit depending on which process (Esy or ES) occurs. With regard to ES, following applied voltage and overcoming the ST threshold of the polymeric solution, rather than the cone jet breaking up into particles (Esy), it becomes unstable. This results in a whipping motion of the liquid between the needle exit and the collection plate, in turn initiating solvent evaporation, yielding polymeric fibers ranging from 2 nm to several micrometers.

Over the recent years, ES has emerged as a versatile method for fiber production for an array of applications[131] (Table 1) including antibacterial delivery,[132] protein delivery, anticancer therapy, and bioengineering.[133]

3.3.1. Protein Delivery

The biggest challenge in the encapsulation and delivery of proteins is maintaining the bioactivity of biomacromolecules throughout the process. Optimization of the EHD system can allow bioactives to be preserved while achieving high EE within fibrous matrices. Electrospun fibrous scaffolds have been developed to encapsulate biomacromolecules to provide structural support as well as to stimulate tissue regeneration.

Model proteins BSA and myoglobin were incorporated into biocompatible PLGA NFs (468 ± 139 nm) to form scaffolds with a loading efficiency of approximately 80%, demonstrating

a useful dual protein delivery system for tissue engineering applications.[134] BSA has also been loaded into electrospun poly(vinyl alcohol) (PVA) NFs with luciferase (a model enzyme). Both molecules retained their bioactivity once electrospun.[135] Ozcan et al. fabricated BSA, globulin, and hemoglobin fiber scaffolds.[136] These high surface area fibrous mats (75, 117, and 220 nm for BSA, globulin, and hemoglobin fibers, respectively) can mimic tissues, producing substrates for regeneration tissue growth. Characterization (thermal, spectroscopic) of scaffolds presented a method for protein scaffolds for biomedical applications.

Li et al. developed PLGA, gelatin, and elastin (PGE) scaffolds which exhibited the ability to support dense cell growth, hence able to deliver high number of cells.[137] Common problems often seen with engineering of macroscopic tissue, such as necrotic cores, was absent from these PGE scaffolds, showing high porosity, facilitating sufficient transport of nutrients as well as waste removal.

3.3.2. Gene Therapy

The ES process has also been directed into the field of gene therapy following success in the protein delivery remit. Process parameters of ES allow sensitive material like DNA to be handled without the integrity of the material being compromised. Fang et al. demonstrated small fibers (50–80 nm) using calf thymus-Na.[138] Shortly after, experiments focused on preparing fibrous materials incorporating lambda DNA, an *E. coli* bacteriophage. Poly(ethylene oxide) (PEO) NFs containing isolated stretched DNA molecules were fabricated within the range of 100 and 350 nm. Modifying the process parameters showed a reduction in the fiber diameter to 550–250 nm.[139] Biodegradable PLGA and PLA-PEG co-block polymer entrapped DNA plasmids to produce NFs (250–875 nm), which showed promising in vitro release with adequate bioactivity.[140]

Small interfering RNA (siRNA) are molecules comprising of two RNA strands, which can be integrated into the "RNA induced silencing complex,"[141] which controls mRNA binding and cleavage. However, the delivery of siRNA has its limitations, both extracellular (degradation, specific cell targeting) and intracellular (endosomal escape, mRNA targeting).[142] The therapeutic application of siRNA often takes the form of nanoparticles; however, for fundamental applications such as tissue regeneration, electrospun fiber production offers a cheap and simple alternative.

Cao et al. encapsulated siRNA in a PCL shell to form polymeric NFs (300–400 nm in diameter) exhibiting controlled release for 28 days under physiological conditions.[143] The siRNA remained bioactive for this duration, showing potential for sustained gene delivery. Copolymeric NFs (caprolactone and ethyl ethylene phosphate) has also been used as a platform to alter siRNA kinetics for siRNA delivery and gene silencing.[144]

3.3.3. Cancer Therapy

Administration of anticancer drugs and delivering a viable amount of drug that will have a therapeutic effect at the site of action is often met with numerous challenges. Physiological conditions (e.g., pH 7) can prevent therapeutic drug concentrations being reached, rendering the administration of drug inadequate. By dissolving the drug into a polymeric solution and producing electrospun fibrous mats, the amount of drug delivered to the site of the tumor as well as its release can be controlled. These mats can be placed directly at the tumor site (for treating the cancer or postsurgery), ensuring virtually that the total amount of drug will be delivered at the desired site. Numerous anticancer drugs have been successfully incorporated into fibers using this method.

Cisplatin is one of the most potent anticancer drugs in medicine. However, it has been extensively used to treat various cancers, including testicular, ovarian, and bladder cancers. Cisplatin-loaded PLA/PLGA fibers were fabricated for the potential treatment of C6 glioma (in vitro studies).[145] The fibers collected had diameters 0.5–1.7 μm, with SEM showing that the fiber fabric consisted of interlocking fibers increasing the strength of the fibrous mats produced. Xie et al. were able to optimize drug loading and fiber diameter by altering the copolymer concentration and EHDA process parameters.

Paclitaxel has also been loaded into polymer fibers to analyze its potential in treating C6 glioma.[146] Paclitaxel was loaded into PLGA fibers (30 nm) with the aid of organic salts. The ultrathin fibers had EE over 90% and were capable of delivering paclitaxel at a sustained rate for more than 60 days. Cytotoxicity tests were carried out to obtain the half maximal inhibitory concentration (IC_{50}) of the drug in this formulation. An IC_{50} value of 36 mg mL^{-1} was observed, a value analogous to Taxol, a commercial paclitaxel formulation.[108]

DOX hydrochloride (DHCl) (an anticancer, bacterial antibiotic active) was a model drug used to demonstrate the feasibility of drug delivery from electrospun PEG/poly(L-lactic acid) (PLLA) (diblock copolymer) fibers using an emulsion rather than a solution.[147] The fibers ranged from 300 nm to 1 μm in diameter with 1–5% drug content within the fibers. Using MTT methods (C6 cell lines), it was established that DHCl could be released without any detriment to its cytotoxicity. The encapsulated DHCl also had the same chemical structure and exhibited comparable antitumor activity to normal DOX, highlighting that the EHDA process does not affect the drug in any way. PEG/PLA and PEO/water-in-oil emulsion was spun to create core/shell fibers, with an average size of 749 μm.[148] The resulting composite fibers exhibited a water-soluble polymer core.

Combining ES with photothermal therapy yielded PLLA NFs (326 ± 63 nm) loaded with DOX-carbon nanotubes that induced cancer cell death along with promoting an increase in diffusion of DOX to the tumor site, consequently showing enhanced inhibitory effect on tumor growth.[149]

3.3.4. Antibiotic Delivery

There are a wide variety of antibiotics available to prevent or treat bacterial infections. However, to maintain their antibacterial activity, constant administration of the drug is required. Failure to do so can result in a concentration lower than the minimum inhibition concentration (MIC), leading to antibiotic resistance. Maintaining the drug concentration above MIC can achieve the desired therapeutic effect over a long period of time, while preventing antibiotic resistance. Incorporating the antibiotics in NFs

has been found to extend the release of drug when ES fibrous mats are applied as wound dressing, accelerating the rate of wound healing as well as preventing infection.

A biodegradable gauze consisting of cefazolin-loaded poly(lactide-co-gylcolide) (PLAGA) NFs has been developed by a research group in USA.[150] Cefazolin is a broad-spectrum bactericidal antibiotic which acts by binding to penicillin binding proteins, inhibiting cell wall synthesis of the cells of that bacterium. Cefazolin is most commonly administered via an intramuscular injection or intravenous infusion, achieving a systemic therapeutic effect. By incorporating cefazolin into NFs, a local therapeutic effect can be achieved, hence faster drug effect. The incorporation of cefazolin produced NFs ranging from 470–490 nm, and by modifying the process parameters, these diameters could be tailored.[150] Fluoroquinolone antibiotics (ciprofloxacin hydrochloride, levofloxacin hemihydrate, or moxifloxacin hydrochloride) have also been embedded in a polymer (poly(L-lactic-*co*-D,L-lactide)/PEG) matrix for wound dressings.[151] ES gave a system with evenly dispersed drug particles along with a release profile with an initial burst release and a subsequent sustained release, a fundamental prerequisite for wound treatment.

More recently, ciprofloxacin was incorporated into various polymeric fibers to achieve a sustained release.[152] Using a blend of PMMA and PVA or chitosan, the release of ciprofloxacin could be optimized over 18 days. Different polymer solutions exhibited different release kinetics; PEO fibers showed high burst effect whereas chitosan fibers demonstrated slow release.

Multi-antibiotic-loaded PLGA fibers have been developed for the prevention of orthopedic implant–associated infections.[153] Fusidic acid and rifampicin were incorporated into PLGA fibers (612 ± 32.2 nm) with EE more than 75%. In vivo evaluation with a rodent model (of implant-associated inflections) demonstrated that 10% FA and 5% rifampicin reduced more than 99.9% of the adherent cells.

3.3.5. Bioengineering

A wide variety of materials have been used in conjunction with ES to develop systems that can create structures able to mimic bone extracellular matrix to fundamentally repair degenerated bone functionality.[154] These ES scaffolds have high surface area and high porosity—characteristics for biomimetic bone tissue engineering.[155] For such applications, a biodegradable, biocompatible material/polymer matrix is required.

Hydroxyapatite (HA) is a biomaterial largely used for bone replacement and regeneration. HA-loaded fibers with average diameters ranging from <100 nm to 20 μm have been produced using various polymeric matrices such as polyurethane,[156] polyvinyl butyral,[157] chitosan,[22] and polycaprolactone.[158] For instance, HA, ibuprofen, and indomethacin were incorporated in an amorphous state into polycaprolactone nanofibers. The fiber sizes were in the range of 400 nm to 20 μm with ≈7–10% encapsulation efficiency. These fibers demonstrated multifunctional biomedical and biomaterial engineering applications.[158]

Chitosan along with collagen has been extensively used in this area due to its biocompatibility and resemblance to structures in the body such as skin, bone, and muscle. Chitosan is a semi-synthetic versatile polymer that has a number of biomedical uses,[159] while collagen is a structural protein found in abundance in animal connective tissue, which has been utilized in treating various bone and skin impediments.[160] Electrospun chitosan and collagen nanofibers have been used to produce novel matrices for wound dressings to encourage/promote skin regeneration. Type 1 collagen, chitosan, and PEO were used to fabricate thin membranes of nanofibers (134 ± 42 nm).[161] SEM images showed that a flow rate of 0.5 mL h^{-1} and AV of 30 kV were the optimized electrospinning processing conditions to obtain nanofibers. In vitro studies showed good biocompatibility, while in vivo animal studies proved that the nanofiber membranes were sufficiently better than gauze and commercial collagen sponge wound dressings with respect to the rate of wound healing.[161]

Chitosan has also been used in conjunction with polyurethane to fabricate loaded fibers to enhance antibacterial activity and mechanical strength of wound dressings. The fiber sheets exhibited strong antimicrobial activity by inhibition of bacterial growth, both gram positive (*Staphylococcus aureus*) and gram negative (*Pseudomonas aeruginosa*), while preventing infection of the wound.[162]

Recent studies have also fabricated nanofibers (combining chitosan with PEO) to encapsulate multicancer-treating drug 5-fluorouracil (5FU) to achieve controlled drug release for biomedical applications.[163] 5FU has also been electrospun into nanofibers for use in tissue scaffolds and novel controlled drug-delivery systems for multiple drugs using nanomicelles,[164] as well as multifunctional PEO fibers containing amphiphilic vesicles for the encapsulation of hydrophobic 5FU and hydrophobic paeonolum.[165] The operating parameters of ES can evidently create systems which can efficiently encapsulate and potentially deliver "environmentally demanding" materials/actives.

Collagen micro- and nanofibers have successfully been used as artificial skin support and as bone scaffolds, highlighting the potential of using ES nanofibers as future material for tissue engineering.[160] Biodegradable poly(esteramide) (derived from L-alanine) scaffolds were fabricated to show the potential for biomedical engineering application. The nanofibers (average of 400 nm) proved to be a strong candidate for vascular tissue engineering.[166]

3.3.6. Miscellaneous Therapeutic Applications

Constant evolution in the EHDA remit is forever exploring new avenues and applications for resultant products. Nanofiber patches have been developed by electrospinning *N,N*-dimethyl formamide (DMF) solutions containing polymers PVA and PCL.[167] The solutions were also loaded with timolol maleate and dorzolamide hydrochloride to assess the capabilities of electrospun fibrous patches for treatment of glaucoma. The patches exhibited approximately 100% entrapment efficiency, with the fibers themselves presenting uniform, narrow diameters (200–400 nm) with smooth surfaces. The introduction/application of electrospun drug-loaded patches in New Zealand white albino rabbits, with induced glaucoma demonstrated a significant reduction of intraocular pressure (IOP) and maintained a reduced IOP for up to 72 h, as opposed to conventional eye drops (<4 h).

Applications of ES have also been implemented in the encapsulation of oil components.[168] Li et al. fabricated borneol–PVP nanocomposites which could be utilized as alternative candidates for novel nano drug-delivery devices. These amorphous fibrous structures were found to have even molecular distribution of borneol with 2% borneol concentration producing the thinnest fibers at 440 ± 140 nm. Due to the hydrophilic nature of PVP, the nanocomposites greatly enhanced the dissolution profile of borneol to 15 s. The interaction between borneol and PVP (hydrogen bonding, confirmed by FTIR) improved the physical stability of borneol; however, the presence of borneol decreased the tensile strength of the fibrous mats. Regardless, these findings highlight the versatility of ES, capable of encapsulating volatile APIs.

Huang et al. utilized electrospinning to develop polymeric fibers to aid the vaginal entrapment of HIV.[169] The resulting polystyrene fibers coated in either poly(allylamine hydrochloride) or dextran sulfate sodium displayed nontoxicity with vaginal epithelial cells, and a significant reduction of injection (associated with CD4(+) TZMb1 cells) was observed, making these polymeric fibers attractive for inhibiting HIV infection topically as opposed to the conventional method of oral treatment.

Electrospinning has also been used to develop scaffolds loaded with antiretroviral saquinavir. Acetalated dextran was found to make a more viable matrix compared to PLGA and PCL. The resulting fibrous matrices were ground down, yielding saquinavir microconfetti, advantageous for tunable long-acting injectables. The microconfetti was capable of releasing the active for more than a week while demonstrating high tissue retention.[170] Acetalated dextran has also been used to encapsulate antiviral resiquimod into fibrous scaffolds, yielding tunable matrices for temporal and sustained drug delivery.[171]

3.4. Coaxial Electrospinning

In the innovative advance in electrospinning technology, coaxial devices have been developed to produce polymeric nanofibers with hollow or core–sheath structures.[172–174] Here, a "multiple solution feed system" encapsulating one solution within another at the capillary exit is used. The device set up for coaxial electrospinning (CES) is similar to that of CEsy with respect to an outer needle and inner needle as required. This technique is particularly advantageous as polymer solutions which are unable to be electrospun can be passed through the inner needle, encapsulating it within a polymeric shell (extruded from the outer needle).[175] For susceptible materials, the shell structure of fibers can protect the core contents while also providing sustained release of the encapsulated material. The first work in producing unique core–sheath structures was demonstrated using a water-in-oil emulsion,[148] but applications have extended to various drug-delivery remits as highlighted in Table 2. CES has been used in developing drug-delivery systems and has initiated various novel devices in nanotechnology.[176–179]

3.4.1. Cancer Chemotherapy

As previously mentioned, cancer therapy drugs currently have limited applications due to low administration efficiency and systemic toxicity.[180] Encapsulation within core/shell fibers can protect the internal healthy biological environment and can release actives at specific sites in a sustained manner. DOX-incorporated PVA/chitosan core/shell nanofibers (280 nm) were produced for the potential application in chemotherapy against ovary cancer.[181] Confocal microscopy showed that the nanofibers were nontoxic to SKOV3 cells (ovarian carcinoma cells) as well, exhibiting that the controlled release of DOX was dependent on the PVA:chitosan ratio. Further assessment demonstrated the adequate performance of the nanofibers via prohibition of SKOV3 cell proliferation, highlighting prospects for chemotherapy of ovary cancer.

Huang et al. from China developed bilayered paclitaxel-loaded poly(lactic acid-*co*-ε-caprolactone) (PLLACL) (core/shell) microfibers to assess cytotoxicity using HeLa cell lines.[182] Paclitaxel was released as a short burst release over 24 h followed by slow release over 60 days. The fibers were found to readily release paclitaxel and inhibit HeLa cell growth efficiently.

More recently, an implantable device which exploited the amphiphilic nature of micelles and broad application of polymeric nanofibers was developed for effective cancer therapy.[180] Hydrophobic DOX was loaded into micelles, and these complexes then made the core of gelatin-shell fibers along with PVA. The development of an implantable device requires reduced drug dose alongside reduced administration frequency and harmful side effects while having maximum efficient therapeutic effect against tumors.

3.4.2. Antibiotic Delivery

Another class of actives which have benefitted successfully from CES are antibiotics. Levofloxacin, a quinolone bactericidal antibiotic, was loaded into chitosan/PCL core/shell fibers.[183] Compared to single needle, the chitosan–PCL nanofiber scaffold presented elevated sustained release of levofloxacin compared to using PCL alone. Such scaffolds could be beneficial for prevention of bacterial infection stemming from postoperative surgery. PCL was also used as a fiber shell material to encapsulate low-molecular-weight antibiotic agent gentamicin sulfate and antioxidant resveratrol (separately) to fabricate double-layered ultrafine fibers (208–1585 nm and 153–1317 nm with 10% Gentamycin and 10% resveratrol, respectively).[184] PCL has also been utilized as a core material in zein-shell NFs loaded with MDZ.[185] Characterization of the resulting electrospun structures presented smooth bead-free NFs, with homogenous distribution of antibiotic throughout the core layer. The hydrophobic nature of zein (as opposed to gelatin) eased initial burst release and prolonged the drug-release period, for over 4 days.

Tetracycline hydrochloride (TCH) is an antibiotic which acts by protein synthesis inhibition. Due to its broad spectrum of antibiotic action, it is commonly used for bacterial infections. CES was used to develop a reservoir-type drug-release device containing TCH.[186] The ultrafine PLLA fibers (150–1312 nm) created fibrous mats which exhibited sustained release of TCH, showing the potential of electrospun fibers for drug carriers or in biomedical applications such as sutures or wound dressings.

3.4.3. Nonsteroidal Anti-Inflammatory Drug Delivery

CES has also been successfully utilized for the fabrication of core–sheath nanofibers containing NSAIDS. The mechanism of such drugs is based on the inhibition of enzymes that help produce prostaglandins. Ketoprofen, a hydrophobic drug used to treat rheumatism, was used as a model drug in a PVP/zein in a polymer/core matrix where homogenously structured fibers had an average diameter of 730 ± 190 nm.[187] DSC and XRD corroborated that all the components were present in an amorphous state. The nanofibers provided an immediate release of 42.3% of ketoprofen followed by a sustained released over 10 h, showing the production of a system capable of biphasic drug release.

Fast-dissolving PVP fibers were fabricated to assess the encapsulation of lipophilic excipients. Quercetin and sodium dodecyl sulfate were used as the core of the fibers and PVP the sheath.[188] TEM showed that the diameters of these fibers were 740 ± 110 nm, while DSC and XRD confirmed that quercetin and sodium dodecyl sulfate were present within the PVP matrix in an amorphous state and evenly distributed. The use of rapidly dissolving PVP here provided a fibrous, fast-disintegrated drug-delivery system capable of preserving active integrity as well as controlled release.

More recently, ibuprofen has been incorporated into drug-loaded fibers[189] as well as into triple-component nanocomposites.[190] Zein (a prolamine protein) was used to incorporate ibuprofen (the core) into *N*,*N*-dimethylformamide fibers (as small as 0.67 ± 0.21 μm). XRD analysis showed that ibuprofen was evenly distributed and present in an amorphous state within the nanofibers.[189] Qian et al. developed triple-component nanocomposites (ibuprofen/PVP/PAN), which had average diameters of 620 ± 120 nm with 10.5% PVP content, providing a novel sustained drug-delivery system.[190]

One major advantage of EHDA is being able to overcome limitations of site-specific targeting, simply by using concentrically arranged conductive needles and optimal materials. Jie et al. explored the encapsulation of indomethacin in PEO/Eudragit core/shell fibers.[191] Indomethacin is a widely used NSAID which is extremely effective in colon cancer treatment. However, numerous studies have shown indomethacin to cause gastrointestinal bleeding and ulceration; hence, colon-targeted formulations can be of value to patients. Using a drug concentration of 9 mg mL^{-1}, NFs with a mean diameter of 740 ± 410 nm were fabricated. The utilization of pH-sensitive Eudragit as shell material prohibited the release in acidic gastrointestinal regions, allowing the mucoadhesive nature of PEO to adhere to the walls of the intestinal tract and providing sustained drug release.

3.4.4. Protein and Peptide Delivery

As mentioned earlier, with regard to the delivery of proteins and peptides, there are some crucial issues with denaturation and maintaining the molecules' bioactivity, all of which can be overcome using CES.

BSA, a model protein, has been frequently used to demonstrate the delivery of proteins using CES. [24,134,192] Electrospun fibrous scaffolds have been developed in which two proteins have been incorporated to provide structural support as well as for the stimulation of tissue regeneration. BSA and myoglobin were integrated into PLGA-PF127 fibrous scaffolds (423 ± 209 nm) with a loading efficiency of around 80%, proving to be a useful dual protein delivery system for tissue engineering applications.[134] BSA was also used in conjunction with rhodamine B and was incorporated into PLLACL nanofibers to develop tissue engineering and drug-delivery carriers.[193]

In a study by Raheja et al. in 2013, core–sheath nanofibers with BSA (545.26 nm), lysozyme (449.44 nm), and insulin (661.88 nm) were fabricated.[192] CES is a simple method where harsh treatment of sensitive bioactive materials such as insulin is not essential, hence providing protection to the biomolecule throughout the entire spinning process. The secondary structure of all the proteins and peptides were retained throughout the CES process, indicating the possibility of a system suitable for cell culture and tissue regeneration.

More recently, Wen et al. used alginate to form the shell of NFS which contained BSA-loaded core for colon-specific controlled release.[194] EHD processing of these materials results in negligible change in the secondary structure of the protein. The core/shell fibers had a core diameter of 175 nm and shell of 280 nm with adequate encapsulation efficiency (75%).

3.4.5. Miscellaneous Applications

One major advantage of the resulting core/shell structures using concentrically arranged nozzles is optimizing/altering shell materials for the development of stimuli-responsive structures—a beneficial product characteristic in biomedical engineering. Wang et al. exploited this concept, developing fibrous PCL structures loaded with magnetic Fe_3O_4. By incorporating a magnetic additive, an externally applied magnetic field can trigger/initiate drug release in addition to acting as image markers, producing fibrous dual-purpose structures.[195]

The incorporation of small concentrations of genipin, a natural cross-linker, into gelatin NFs overcame issues with morphological stability upon exposure to aqueous surroundings.[196] The electrospun fibers maintained stabilization, with in vitro studies demonstrating that the mats supported human primary chondrocyte culture in turn promoting cell differentiation.

Despite significant development in percutaneous coronary intervention, restenosis and stent thrombosis are still hurdles which need to be considered. Boodagh et al. developed PEG methacrylate/poly(L-lactide acid) fibers, which increased stem cell secretory factors, as a result of platelet and smooth muscle cell attachments, enhancing endothelial proliferation.[197]

The complexity of skin structure in turn poses challenges to the wound healing process. Fabrication of fibrous scaffolds with high active loading can expedite approaches in tissue regeneration, overcoming this hurdle. Shoba et al. exploited CES principles and developed core/shell fibers for controlled delivery of enzyme bromelain and bioactive salvianolic acid B (Sal B).[178] The biomimetic PCL-core and PVA-gelatin-shell scaffolds successfully enhanced proliferation of keratinocytes and inhibited bacterial growth in vitro. The incorporation of bromelain in the shell and Sal B in the core resulted in a burst release of the

enzyme and a sustained release of Sal B, demonstrating accelerated in vivo wound healing.

3.5. Combinatorial Electrospraying and Electrospinning

Using Esy in conjunction with ES can yield a generation of new nanocomposites. Combining particles and fibrous mats can be used to develop systems with complex release kinetics with multiple functionalities (multidrug release).

Lavielle et al. used simultaneous Esy and ES of PEG and PLA solutions to produce MPs and NFs.[198] The composites self-organized into hierarchical honeycomb-like structures with pore sizes ranging from few to several hundred micrometers. Here, the particles could be selectively leached, leaving the multilevel matrix of NFs appropriate for biomedical applications.

A research group in Italy developed electrically conductive membranes spinning polymeric solutions and simultaneously spraying multiwall carbon nanotubes (MWCNTs).[199] The fibrous mats, between 80 and 100 mm wide, with fibers ranging between 100 nm and 10 μm show promise as a contender for charge prevention in filter media.

3D scaffolds with the ability to mimic extracellular matrices were generated using patterned ES–Esy.[200] The PCL scaffolds exhibited enhanced cell attachment with continuous cell proliferation over 21 days on novel scaffolds. Even distribution of bone minerals (Ca_2) confirmed by EDX analysis shows that patterned scaffolds could be promising for proper bone graft substitution in bone tissue regeneration. Nanohydroxyapatite (nHA) was electrosprayed on electrospun gelatin scaffolds for another potential substrate in bone tissue regeneration.[201] Characterization involving cell proliferation and field emission scanning electron microscopy (FESEM) showed that the combination of Esy nHA particles and ES gelatin fibers made for promising substrate in bone tissue regeneration.

A novel setup of using counter-charged nozzles was used to combine particles and fibers.[202] Lysozyme (inner) and PLGA (outer) solutions were infused through a coaxially arranged positive voltage generation while PLA was expelled through a negative voltage generator. In situ combination of Esy and ES in counter-charged nozzles resulted in a neutralization at the collection plate, providing a novel method to engineer scaffolds with complex functionalities for tissue engineering. The core/shell particles alone cannot provide structural support; incorporation of electrospun fibers can increase active loading and hence provide sustained release while providing sufficient support as scaffolds.

3.6. Near-Field Electrospinning

Controlled printing and patterning via droplet deposition at adequate resolutions is currently a hurdle in nanotechnology. Current methods such as nanolithography possess the potential to achieve nano patterns but are often disregarded due to elongated processing and high costs.

The ability to generate and deposit micro/nano particles at high resolutions has propelled research based on near-field electrospinning (NFE) in recent years. NFE is a manufacturing process that allows micro/nano patterns to be printed onto surfaces using electrical field as the driving force to jet ink through conductive nozzles, allowing the printing process to be controlled by altering the voltage potential. The ions present in the solution being ejected are attracted toward a substrate, with the aid of electric field. This causes the cone jet to deform leading to instability. The release of the droplets occurs at the cone apex.[203]

The device setup similar to Esy and ES, with an added high-speed camera (for process monitoring) and the liquid is pulled through the system rather than infused, as with Esy and ES; but is pulled through the system. Two methods of EJP have been established based on the type of applied voltage: continuous printing (CP) and on-demand printing (ODP). CP utilizes a constant voltage, while for ODP, a pulsed voltage is necessary. CP is often associated with high costs due to ink wastage as a result of constant expulsion of ink. CP can also observe destabilization of the cone jet, resulting in polydisperse patterns. ODP is often favored due to the jet expulsion being controlled; ink is only printed when required, increasing drop accuracy. Chen et al. utilized the basic EHD aspect to generate and deposit sulfate latex spheres from a deionized water suspension accurately using "drop-and-place" deposition.[204] Colloidal particles of 2 μm were achieved using a 50 μm nozzle at an applied voltage of 12 kV and pulse duration of 7.5 ms.

NFE is seen as a competitive alternate printing method due to its speed, reliability, and high resolution capabilities (100 nm)[205] compared to ink jet printing (10–30 μm) or piezoelectric printing (10–20 μm). E-jet devices use significantly larger capillary nozzles leading to reduced capillary blockage leading to easier processing of solutions, especially viscous liquids.

Although the method of inkjet printing was originally intended for computer printing applications, advancements in technology has widened the application of ink jet printing to drug discovery, tissue engineering, and material science with an array of materials already processed, including metallics (e.g., silver,[206–211] copper,[212–214] gold[215,216]), biomaterials,[217–221] and ceramics.[222,223]

For example, NPs of HA were suspended in an ethanol-based suspension and was subjected to an electric field. The droplets were deposited according to a programmed topography, yielding pattern tracks as small as 50 μm.[220] This application of NFE (utilizing HA NPs) has also extended to the regulation of human osteoblast cell attachment and orientation,[217] as well as for the analysis of the potential for osteoconduction of implants.[221]

The capabilities of this technology have also extended to forming/producing films and architectures for tissue and biomedical engineering. Nanocomposite biopolymer scaffolds for potential organ development were generated, where a 3D print-patterning device yielded threads less than 50 μm according to a predetermined pattern,[224] while direct printing of PCL with nano-HA nanocomposites deposited small, predetermined structures (less than 5 μm), which could be very advantageous in biomedical engineering.[225]

The precision in deposition with EJP has also been beneficial in the fabrication of fibrous scaffolds for bone tissue regeneration. 3D bioceramic-based fibrous scaffolds were fabricated by Kim et al. using PCL and α-TCP.[222] Exposure of these

scaffolds to MC3T3-E1 preosteoblasts demonstrated enhanced cell attachment, proliferation, and cell differentiation, showing the potential of ceramics and NFE in bone regeneration.

Wang et al. have developed patterned antibiotic-loaded PVP/PEO fibers using NFE, successfully producing various patterns including parallel lines, arcs, and grids.[226] Such patterns are ordinarily difficult to produce using conventional ES methods. The resultant printed composite fibers (700 nm–5 μm) exhibited drug TCH release for over 5 days, results that mimic existing polymer-based systems.[227] The same research team also prepared TCH-loaded 3D film patches using the same polymeric materials.[228] Similar results were yielded with TCH being released over 5 days from PCL-PVP patches and the release being slower than pure PCL and PVP, meeting crucial demands where personalized approaches were essential.

Revolutionary advancement in NFE has yielded a process in which NFs are written in a continuous, accurate, and controlled manner using a WD less than 5 mm. In dual-nozzle near-field electrospinning, an important fact to note is that the effect of the applied electrical force is negligible as the Coulomb forces are the dominant force. This characteristic was exploited to successfully produce ethylene oxide aligned NFs using two adjacent needles.[229] Wang et al. found that by increasing the voltage and/or electrode-to-collector distance, the deposition distance increased. The outcomes of this study can be used to help achieve more optimized deposition distance and dense NFs.

With the novel capability of patterning as well as film deposition along with modern technology development (multi-needle, needleless), the full potential of NFE is yet to be exploited.

3.7. Recent Technological Advances

Table 3 summarizes the following advances in EHDA from a technological viewpoint, emphasizing the results yielded from the studies with regard to size and outcomes.

3.7.1. Multiaxial EHDA

After the success of utilizing coaxial arrangement of nozzles to develop core/shell structures, advances in EHD technology have now made multilayered microstructures a possibility using immiscible liquids. This technological approach can be used to produce structures loaded with multiple actives, yielding a dual-purpose device. There are many advantages for multilayered particles or fibers, most critically protecting susceptible materials with the outer sheath. The outer shells can also serve as the release-limiting layer, providing sustained release of encapsulated API in the intermediate layer or core. Due to the complexity of the process (due to the prerequisite of immiscible liquids),[230] this branch of EHDA has not been fully researched/exploited.

Multiaxial Electrospraying: A tri-needle EHDA device developed by Ahmad et al. demonstrates the production of various morphological particles (β, δ).[31] Multilayered bubbles consisting of air (inner-most needle), glycerol (intermediate needle), and olive oil (outer-most needle) were generated. Optimized conditions (6–8 kV; flow rate: air = 250 μL min^{-1}, glycerol = 30 μL min^{-1}, olive oil = 50 μL min^{-1}) resulted in concentric encapsulation of air, with SEM images showing apparent visible layers. Ahmad et al. went on to use a more viscous solution (high-molecular-weight PEO), rather than glycerol, leading to the production of multilayered fibers (100–200 μm in width) containing trapped bubbles of air. This study also highlighted the importance of spacing between the concentrically arranged needles; encapsulation efficacy can be compromised if there is direct contact between adjacent needles.[31]

A triple-needle device was also developed by Labbaf et al. which produced trilayered nanoparticulate structures (220–320 nm).[231] SEM and TEM images indicated spherical morphologies with three distinct layers: PLGA (outer needle), polycaprolactone (intermediate), and PMSQ (inner needle). The same group extended this study and developed a novel four-needle EHD device, obtaining four-layered nanoparticles consisting of PLGA, polycaprolactone, PEG, and PMSQ.[232] TEM images showed that the multilayered particles were spherical in shape and of an average size of 620 ± 150 nm. Various dyes were added to each polymer solution and were electrosprayed. Different release rates and percentage release of the dyes were observed due to the difference in thickness of each layer—an advantage of using polymeric layering—controlled release of more than one "drug."

PLGA and poly(styrenesulfonate) (PSS) particles containing several drugs (budesonide, epigallocatechin gallate [EGCG]) have been successfully electrosprayed using a tri-capillary system.[233] Trilayered particles, around 500 nm in diameter, were produced using flow rates of 1.0, 2.0, and 10 μL min^{-1} for the inner PSS solution, intermediate PLGA solution, and outer PSS solutions. Lee et al. found that the thickness of layers within the particles could be controlled via varying the feed rates of each individual solution. Modifying the composition and thickness of the multiple layers, the trilayered structures achieved multidrug release compared to dual-capillary device configuration.

More recently, a coaxial tri-needle system was utilized to engineer multiagent compartmental particles capable of dual-imaging modality.[234] The magnetic polymer yolk–shell particles (made up of magnetic iron oxide NPs) demonstrated triggered active release upon modifying the frequency of an external auxiliary magnetic field. The ability of these particles to be loaded with multiple active agent, to have temporal drug release system, and to have diagnostic features demonstrates their potential as multifunctional theranostic agents.

3.7.2. Multiaxial Electrospinning

An issue with electrospinning is the level of fiber production. To overcome this, research has extended toward multi-needle devices.[235] Utilizing a multiaxial electrospinning system is a cost-effective, convenient, one-step method to fabricate specific structured nanofibers at a high production rate.[236]

Biodegradable multilayered fibers have been fabricated by Lui et al. using triaxial (three-needle) electrospinning setup.[237] PCL (intermediate layer) and gelatin (sheath and core) were electrospun, and fibers of 25 μm were generated, as shown by Field Emission SEM (Fe.SEM) showing the ability to prepare materials for application in biotechnology.

Table 3. Summary of selected recent technological advances in EHDA.

Method	Matrix	Active	Size [nm]	Comments	Reference
Coaxial electrospraying (three needle)	PLGA (outer needle), PCL (intermediate), PMSQ (inner needle)	–	0.22–0.320	Spherical nanoparticles with three distinct layers were yielded; the multicompartment characteristic of these structures can aid in the release of multiple API alongside controlled release.	[231]
Coaxial electrospraying (three needle)	PCL, silicone oil	Various probes	0.5	A novel three-needle coaxial system engineered magnetic yolk–shell particles capable of hosting and delivering multiple probes.	[234]
Coaxial electrospraying (four needle)	PLGA, PCL, PEG, PMSQ	Dye	$620 \pm 1500.620 \pm 0.150$	These multilayered particles were found to be spherical in shape with each layer possessing different thicknesses. As a result of this, different release rates of incorporated dyes were observed, highlighting the prospective uses for multiaxial electrohydrodynamic processing.	[232]
Coaxial electrospinning (three needle)	PVP (core), PCL (intermediate and sheath)	Key acid blue, key acid uranine	0.648	These trilayered fibers provided a biphasic release profile, with the intermediate layer acting as the release-limiting layer retarding probe release from the core.	[238]
Coaxial electrospinning (three needle)	PVP (core), PCL (intermediate layer), cellulose acetate (shell)	Nisin	—	Nisin was encapsulated in a hydrophilic core in an attempt to prolong its release. The electrospun fibers provided antimicrobial defense for up to 7 days against gram-positive bacteria.	[239]
Multi-needle electrospinning	PEO	—	As small as 200	7, 19, or 37 needles were utilized. Preliminary studies demonstrated that the spatial location of needles in a hexagonal pattern aided the formation of uniform electric field at the needle tip.	[245]
Multi-needle electrospinning	PLGA	—	0.65	A circular and rectangular plate was used to analyze the ability of four adjacent needles to spin fibers. The circular configuration was more easily controlled with uniform particle size distribution as a result of stable cone jet formation at each nozzle tip.	[246]
Needleless EHDA	PEO	—	0.2–0.8	Stable jet formation was achieved using magnetic field in conjunction with electric field. Perturbance of the PEO layers due to applied magnetic field increased fiber production rate.	[249]
Needleless EHDA	PVA	—	–	A conical wire was utilized as a spinneret, producing much thinner fibers compared to single-needle electrospinning.	[270]
Novel nozzle design, angular nozzle	PCL	Indomethacin, Sudan Red G	As small as 41.2 ± 7.5	Modified nozzle design (angular nozzle tips) found to enhance stable jetting of liquid. Optimizing process parameters and physical liquid properties resulted in tunable drug release.	[261]
Sawtooth-type slit nozzle	Ethanol	—	18–22	Each tooth in the parallel slit possessed a stable cone jet which produced a high throughput of monodispersed droplets.	[263]
Nonconcentric needles	PLGA, PMMA, modified PMMA and PLGA	Probe	0.423 ± 0.291	Co-jetting of liquid produced Janus particles with optimized morphology and compartment loading. The particles here exhibited site-specific targeting capabilities.	[259]

(*Continued*)

Table 3. Continued.

Method	Matrix	Active	Size [nm]	Comments	Reference
Modified nozzle geometry	Tris(8-hydroxyquinolinate) aluminum	—	As small as 6.8	Five different processing nozzles were analyzed, each tip with increasing number of protrusions (1–4). At each protrusion, a stable meniscus formed; hence, the more protrusions there are, the higher the throughput.	[262]
Near-field electrospinning	PCL, α-TCP	—	341.9 ± 18.9	Exposure of bioceramic scaffolds to preosteoblasts exhibited improved cell proliferation and differentiation, aiding bone regeneration.	[222]
Near-field electrospinning	PVP, PEO	TCH	0.7–5	Development of printed antibiotic-loaded 3D films demonstrated drug release over 5 days, beneficial for personalized drug delivery.	[227]
Near-field electrospinning	PCL	nano-hydroxyapatite	<5	Direct printing of PCL-HA was successfully carried out, producing predetermined patterned threads for bioengineering.	[225]

HA, hydroxyapatite; PCL, polycaprolactone; PEG, polyethylene glycol; PEO, poly(ethylene oxide); PLGA, poly(lactic-*co*-glycolic) acid; PMMA, polymethyl methacrylate; PMSQ, polymethylsilsesquioxane; PSS, poly(styrene suffocate); PVA, polyvinyl alcohol; PVP, polyvinyl pyrrolidone; α-TCP, alpha tricalcium phosphate; TCH, tetracycline hydrochloride.

PCL has also been used for the fabrication of three-layered structured nanofibers containing two drug-mimicking dyes (key acid blue [KAB] and key acid uranine [KAU]) using a triaxial system for the application in wound treatment.[238] These nanofibers (648 nm) consisted of a hydrophobic core (PVP/KAB), an intermediate layer (PCL/chloroform), and a hygroscopic sheath (PCL/KAU), which exhibited sustained released of the "drug" from the core and a burst release from the sheath. SEM microphotographs demonstrated uniform layer morphologies with no bead formation, highlighting the potential use of these dual-drug triaxial nanofiber membranes for wound treatment, externally and internally.

Han et al. developed trilayered fibers in an attempt to prolong the release of antimicrobial nisin.[239] The active was encapsulated in a PVP core which sat at the center of NFs with a PCL intermediate layer (release-limiting layer) and cellulose acetate shell. These triaxial fibers provided antimicrobial defense for up to 7 days, with more than adequate antimicrobial activities against gram-positive bacteria *S. aureus*. The entrapment of nisin within multilayered NFs is highly beneficial to various applications, including but not limited to food packaging and cancer therapeutics.

3.7.3. Multi-Needle EHDA

The use of several needles and syringes within the process allows the fabrication of complex fibrous mats such as tissues, electrospun from a multijet. This system is more complex than single or coaxially arranged needles. Rather than concentric needles, they are placed adjacently to each other. While this setup can scale up fiber production, there can be complications due to the result of repulsion that may occur between similarly charged jets. Multi-needle systems require well thought out configuration of needles in order to optimize electrospinning productivity. With single-needle EHDA, the issue of needle geometry (location, spatial location) is not of concern. Introduction of more needles can cause disturbance with jet stabilization resulting in the production of irregular morphologies. Extended multinozzles are the most common configuration for multinozzle Esy. They are mainly made of silicone[240,241] but some have also been seen to be made from polymers[242] and metals.[243]

Deng et al. microfabricated a device with high-density nozzle packing (250 needles cm^{-2}) etched into silicone which enables a high throughput of droplets, developing a novel device with scale-up potential,[241] while Lhernould and Lamert cultivated an 8-nozzle Esy system. Here, the space between the nozzles was greater than the space between the nozzle and extractor, allowing each Esy to act independently, again highlighting the spatial location of nozzles to be a limiting factor in multi-needle EHDA.[244]

An electrospinning system consisting of sets of three needles (positioned in the shape of an equilateral triangle) with various numbers of needles (7,19, 37) arranged around these to form a regular hexagon shape was devised by Yang et al.[245] SEM images indicated mean PEO nanofiber diameters of 400 nm (7 needles) and 200 nm (37 needles). Preliminary simulation tests specified that using outer needles in a hexagonal shape assisted in the creation of a uniform electric field near the tips of the needles. Due to this, thinner fibers were generated in the main study using PEO solutions. The more needles used in this system, the shorter the working distance needed to be to yield successful structures. Needles can be configured in various ways, for example, circular, triangular, or hexagonal, as demonstrated by Yang et al.[245]

Due to the use of electric force in EHD processing, the spatial organization of the nozzles through which the liquids are fed through is crucial (due to charge buildup and/or repulsion). Parhizkar et al. studied the ability of four separate needles to spin fibers when attached to a circular and rectangular metallic plate.[246] This novel multi-needle EHDA setup produced particles at higher rates when compared to single-needle Esy. A stable Taylor cone jet had formed at each nozzle tip with each plate, allowing the controlled production of uniform particles; however, the circular plate configuration was more easily controlled with more uniform size distribution.

3.7.4. Needleless Electrohydrodynamic Processing

Needleless EHD processing is a cost-effective, simple process which can be used for high fiber production rate with the process being dependent on the jet forming from an open liquid surface. By relying on external forces such as magnetic field, gravity, or high air pressure, the liquid forms conical spikes once the spinnerets are employed.[247] There is high efficiency when using this system and eliminates the problem of clogging up the device. This process is also more cost-effective for mass production.[248] The idea of using a combination of magnetic field and electrical field to initiate the jet formation was proposed by Yarin and Zussman in 2004.[249] Numerous PEO spikes were generated when the magnetic field was applied, and once the applied voltage reached a threshold, multiple jets protruded toward a grounding electrode, with the disturbance of the PEO layer (as a result of the magnetic field and ferromagnetic suspension) of the NFs (200–800 nm) leading to a 12-fold enhancement in NF production rate.

Wang et al. developed a needleless system using a conical metal wire coil as the spinneret for the fabrication of PVA nanofibers. Compared to single-needle electrospinning, the fibers produced were much finer and thinner when produced on a large scale.[250] The needleless system was also used to produce fine PVA nanofibers using a rotating cylinder nozzle and rotating disk. The fibers generated using the rotating disk were much finer than those by the cylinder nozzle.

Tang et al. have proposed a device which utilizes a metal roller spinneret upon which the polymer solution is ejected onto.[251] Once the voltage is applied, multijets are ejected from the polymer solution surface. In comparison to single-needle devices, this novel setup heightened fiber production by 24–45 times. Due to simplicity when scaling up and ease of set up and production, various patents have been issued for this technique, showing its versatility.[252–254]

More recently, a needleless coaxial system has been developed to create core/shell NFs for the time-regulated release of APIs.[255] A novel weir spinneret was utilized here which enabled the production of bilayered NFs, which furthered the research by Forward et al. who found that using a rotating wire electrode could form bi-liquid structures.[256]

3.7.5. Novel Complex Nozzle Systems

A novel nozzle-less emitter device was developed by Bocanegra et al. which utilized orifices in place of stainless steel needles to achieve a stable cone jet.[257] The use of pores (37 in total, in hexagonal planar) to atomize liquids improved the stability of the cone jet with spatial location or diameter of the pores having negligible effect on the electrical stability of the cone jet. Zhang et al. has developed a horizontal flute-like multipore device to generate biodegradable PCL MPs.[258] Jet bending due to spatial locations of the pores resulted in structures with various morphologies. By altering these locations, jet stability was regained, yielding a high-throughput process.

Moe et al. designed a device in which rather than utilizing coaxially arranged nozzles, converging nozzles were used to produce composites as segmented compartments.[259] This configuration generated Janus particles with varied compartment sizes and loading volume with multifaceted functions. Aligned needles have also been used by Rahmani et al. to develop Janus particle systems which have been used to produce particles where the shape and segment loading volume can be modified, advantageous for personalized specific drug delivery.[260] A nonconcentric spinneret which consisted of an angled aligned nozzle was developed by Zhang et al.[261] The novel system produced distinct Janus particles using relatively high electric field. By optimizing the process, Janus particles with specific morphological features were yielded, improving the capabilities of such particles for tunable drug release.

A research group from Japan studied the effects of the geometric shape of nozzle tip on the Esy process when fabricating thin films.[262] Five different processing nozzle tips were explored, each with a different number of projections. The device setup using a high number of projections produced more uniform, smaller droplets with decreased size distribution. At each protrusion, a stable meniscus formed, resulting in high throughput. Upon increasing the number of protrusions (1–4), the surface roughness of the tris(8-hydroxyquinolinate) aluminum films was improved (32.5– 6.8 nm), demonstrating how the manipulation of the geometric shape of nozzle tip can determine the deposition of organic thin films.

Kim and Kim developed a sawtooth-type slit nozzle where each sawtooth tip generated monodispersed structures ranging between 18 and 22 μm.[263] They found that each parallel slit on the device houses a stable cone jet. Due to the variation between the tip being negligible (<6%), the modified nozzles can be seen as corresponding spraying nozzles. This complex device setup enables the production of droplets with high throughput, producing large areas of thin films for surface coatings. More recently, multi-tip stabilizing emitters have been developed to enable increased production rates of particles.[264]

Figure 3g–l demonstrates various nozzle designs that have shown great potential, ranging from the simplest to the more complex developments, while **Figure 4** summarizes the potential of EHD processing to engineer nonconventional structures.

3.7.6. Pressurized Electrospinning

Continuous evolution in pharmaceutical technology has driven the approach to electrospinning toward various developments, one of which involves an introduction of pressure to the electrospinning system. Applying pressure to the system once the liquid solution has infused through to the single needle encourages/enhances stretching of the polymeric solution at the needle exit.[265] Jayasinghe and Suter found that this pressure-driven approach to electrospinning was comparable to the conventional electrospinning process, yielding a direct fiber spinning process with more advantages.[266] The need for high-intensity electric field is eradicated, and highly conductive materials can benefit from this process.

Wahyudiono et al. generated PVP fibers under pressurized CO_2 (8 MPa) using DCM as the solution solvent.[267] At room temperature, the fibers yielded were wet. However, dry fibers

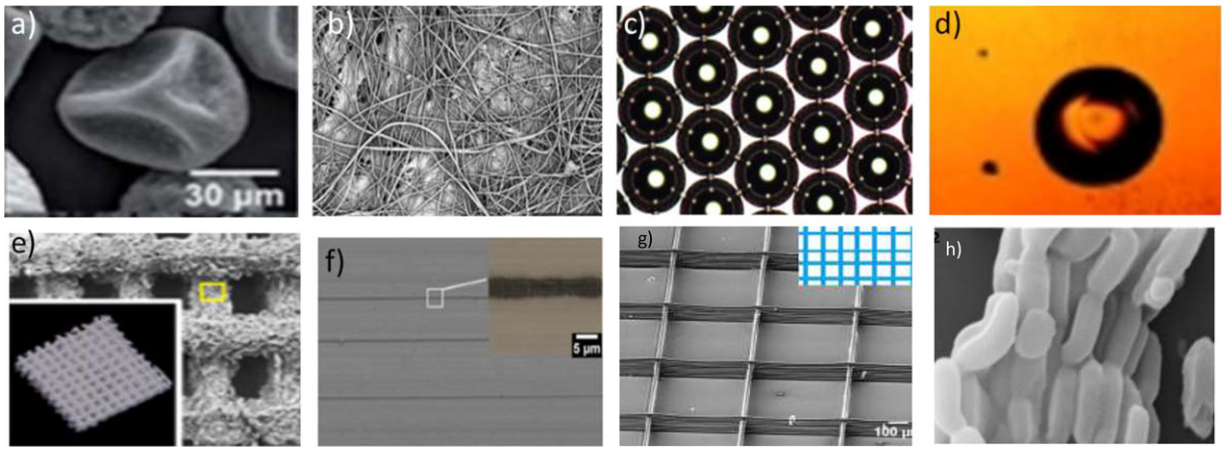

Figure 4. Examples of nonconventional EHDA engineered structures. a) SEM image exhibiting the novel morphology of dual-drug (NSAID indomethacin and model dye Sudan Red G)-loaded PCL Janus particles; Reproduced with permission.[261] Copyright 2015, Taylor & Francis Online. b) SEM image which demonstrates the successful incorporation of C2CI2 cells into PVDFhfp scaffolds by showing cells spread under a layer of electrospun fibers in layer-by-layer process; Reproduced with permission.[285] Copyright 2016, RSC Advances. c) Optical microscope imagery showing glycerol–air microbubbles produced using EHD technique at 6 kV; Reproduced with permission.[122] Copyright 2014, Royal Society. d) Coaxial tri-needle encapsulation resulted in trilayered bubbles with an air core, glycerol intermediate layer, and olive oil shell; reproduced with permission.[31] Copyright 2008, Nature. e) SEM records showing the successful engineering of ceramic (a-TCP/PCL) grids using EHD printing; Reproduced with permission.[222] Copyright 2017, Nature. f) Electron micrograph showing the potential of EHD printing with the fabrication of printed antibiotic-loaded PEO/PVP patches; Reproduced with permission.[226] Copyright 2016, Elsevier. g) Controlled pore-size-based drug release through printing. Reproduced with permission[228] Copyright 2017, Nature. h) Loaded porous materials via EHDA; reproduced with permission.[72] Copyright 2018, Elsevier.

were generated following isolation of polymeric fibers from pressurized CO_2. Depressurization aided solvent removal from the samples, demonstrating the potential of a pressurized electrospinning process.

The same research group from Japan used the same process to develop hollow PVP fibers (2–4 µm pores), with low pressures yielding solid fibers and pressures at approximately 8 MPa yielding balloon-like structures.[268] More recently Wahyudiono et al. generated PMMA multi-hollow fibers under pressurized CO_2 (4–6 MPa), and fibers with diameters between 4 and 16 µm yielded under subcritical CO_2.[269]

3.7.7. Centrifugal Electrospinning

Centrifugal electrospinning is another development that has been established to overcome various limitations of conventional electrospinning such as low production rates from a commercial view point and failed/limited ability to respond as biological fibrous materials (e.g., tendons).[270] Wang et al. attempted to overcome/bypass these limitations by developing a multi-compartmental centrifugal electrospinning device.[271] Multiple formulations were infused through the system and expelled via a rotating spinneret (200–400 rpm). By exploiting electrical and centrifugal forces and using modified spinneret, blended and multialigned fibers could be engineered using multiple materials. This exploitation also enhanced the fiber production rate (120 g h^{-1}) while potentially providing improved capabilities of mimicking biological tissues. The same research team also assessed the mass production of antibiotic-loaded aligned PVP fibers using centrifugal electrospinning.[272] Antibiotic TCH was embedded within the fibers with optimized electrospinning process operating at production rates favorable in industry (120 g h^{-1}).

Edmondson et al. demonstrated the versatility of centrifugal electrospinning system with polyvinylidene fluoride, chitosan (natural polymer), and PEO (synthetic polymer).[273] The motorized spinneret here produced highly aligned fibers at a high degree of uniformity on a large scale.

Kancheva et al. developed a centrifugal electrospinning system which engineered PAN fibrous mats, 2200 cm^2 in area, in less than 20 min using up to four nozzles.[274] The use of more nozzles found to increase the strength of the mats, with the multinozzle setup reducing production time considerably.

3.7.8. Cell Electrospinning

Cell electrospinning is a biotechnological process which involves encapsulating cellular components in polymeric matrices using EHD technologies, with the resulting structures being considered "biologically active." Incorporation of living cells into electrospun fibrous mats can result in highly dense cells, uniformly distributed among the polymer matrix. This overcomes issues of downstream steps, for example, cell seeding and handling of materials, hence reducing development and manufacturing time.[275]

Some of the earliest works in this field found by Esy smooth muscle cells in conjunction with electrospinning poly(ester urethane) urea (PEUU) produced a biodegradable fibrous mat with integrated high-density cells.[276] The same research group elaborated on these results and fabricated electrospun synthetic microintegrated blood vessels using PEUU, overcoming challenges such as time consuming in vitro cellular infiltration with the polymeric matrix. The biodegradable electrospun fibers mimicked

the mechanical behaviors of intrinsic arteries, highlighting the potential of ES in fabricating biologically active tissues for blood vessel replacement.[277]

A research group from London, UK, explored the potential of developing a bioactive scaffold using coaxial arrangement. Microthreads containing living biosuspension core and poly(dimethylsiloxane) shell were yielded with no apparent damage to the incorporated cells.[278] In the last decade, the capabilities of cell electrospinning, which has been extensively researched, yielded a wide range of biologically active and functionalized scaffolds for an array of applications.[275,278–283] For example, Ehler and Jayasinghe immobilized cardiac monocytes within fibers with the aim that these scaffolds could potentially aid in the repair of cardiac tissue or even mimic fully functioning cardiac tissue for replacement of damaged tissue.[284]

More recently, a cell-laden hybrid biograft was developed to act as a carrier for in situ delivery of cells.[285] The layered graft was achieved by alternating electrospinning poly(vinylidene fluoride-cohexafluoropropylene) fibers and Esy murine myoblast cells. The fabrication of 3D biomimetic tissue using this method again overcomes the major limitations of process time and cell infiltration.

4. Concluding Remarks

Fundamental developments in EHDA have yielded complex nanostructures with multifaceted release kinetics with countless applications in the drug delivery and bioengineering/biomedical arena. The simplicity and economic value of the atomization process is greatly advantageous, and tuning key process parameters and physical liquid properties has helped develop innovative devices and EHD setups (e.g., multiaxial, needleless, printing); all yielded promising results. From delivery of large biomacromolecules (e.g., proteins, enzymes) to broadly used drugs such as antibiotics and NSAIDs to fabrication of scaffolds for tissue regeneration, EHDA has presented itself as a robust and on-demand process with high-throughput systems.

Acknowledgements

The authors thank the EPSRC EHDA Network and The Royal Society for their support.

Conflict of Interest

The authors declare no conflict of interest.

Keywords

biomaterials, electrohydrodynamic atomization, electrospinning, electrospray, fibers, particles, pharmaceuticals

Received: February 22, 2018
Revised: August 31, 2018
Published online: December 20, 2018

[1] P. Mehta, R. Haj-Ahmad, M. Rasekh, M. S. Arshad, A. Smith, S. M. van der Merwe, X. Li, M. Chang, Z. Ahmad, *Drug Discov. Today* **2017**, *22*, 157.
[2] A. Perez, R. Hernandez, D. Velasco, D. Voicu, C. Mijangos, *J. Colloid Interface Sci.* **2015**, *441*, 90.
[3] M. Zamani, M. P. Prabhakaran, S. Ramakrishna, *Int. J. Nanomed.* **2013**, *8*, 2997.
[4] Y. Xia, D. W. Pack, *Chem. Eng. Sci.* **2015**, *125*, 129.
[5] P. Mehta, L. Justo, S. Walsh, M. S. Arshad, C. G. Wilson, C. K. O'Sullivan, S. M. Moghimi, I. S. Vizirianakis, K. Avgoustakis, D. G. Fatouros, Z. Ahmad, *J. Drug Target.* **2015**, *23*, 305.
[6] J. M. Grace, J. C. M. Marijnissen, *J. Aerosol Sci.* **1994**, *25*, 1005.
[7] W. Kim, S. S. Kim, *Polymer* **2011**, *52*, 3325.
[8] W. Gilbert, *De Magnete, Magneticisque Corporibus, et de Magno Magnete Tellure*, Wolfgang Lockmans, Stettin **1628**.
[9] K. Q. Tang, A. Gomez, *J. Colloid Interface Sci.* **1995**, *175*, 326.
[10] G. Taylor, *Proc. R. Soc., Ser. A* **1964**, *280*, 383.
[11] J. Zeleny, *Phys. Rev.* **1914**, *10*, 1.
[12] J. Zeleny, *Phys. Rev.* **1917**, *10*, 1.
[13] H. Khan, P. Mehta, H. Msallam, D. Armitage, Z. Ahmad, *J. Drug Target.* **2014**, *22*, 790.
[14] P. Mehta, A. A. Al-Kinani, R. Haj-Ahmad, M. S. Arshad, M. Chang, R. G. Alany, Z. Ahmad. *Eur. J. Pharm. Biopharm.* **2017**, *119*, 170.
[15] W. J. Morton, *US705691 QA*, **1902**.
[16] L. Rayleigh, *Proc. London Math. Soc.* **1878**, *s1–10*, 4.
[17] J. F. Cooley, US Patent 692,631, **1902**.
[18] A. Formhals, *US1975504 A*, **1934**.
[19] A. Formhals, *US Patent 2,123,992*, **1938**.
[20] J. Doshi, D. H. Reneker, *J. Electrostat.* **1995**, *35*, 151.
[21] H. B. Zhang, S. N. Jayasinghe, M. J. Edirisinghe, *J. Electrostat.* **2006**, *64*, 355.
[22] M. E. Frohbergh, A. Katsman, G. P. Botta, S. C. L. P. Lazarovici, U. G. K. Wegst, P. I. Lelkes, *Biomaterials* **2012**, *33*, 9167.
[23] K. Tonsomboon, D. G. T. Strange, M. L. Oyen, *Annual Int Conf IEEE Eng Med Biol Soc.* **2013**, 6671.
[24] H. L. Jiang, Y. Q. Hu, Y. Li, P. C. Zhao, K. J. Zhu, W. L. Chen, *J. Controlled Release* **2005**, *108*, 237.
[25] A. Jaworek, A. Krupa, *J. Aerosol Sci.* **1999**, *30*, 873.
[26] J. Yao, L. K. Lim, J. Xie, J. Hua, C. Wang, *J. Aerosol Sci.* **2008**, *39*, 987.
[27] Y. Wu, R. L. Clark, *J. Biomater. Sci., Polym. Ed.* **2008**, *19*, 573.
[28] M. M. Hohman, M. Shin, G. Rutledge, M. P. Brenner, *Phys. Fluids* **2001**, *13*, 2221.
[29] M. J. Laudenslager, W. M. Sigmund. *Am. Ceram. Soc. Bull.* **2011**, *90*, 22.
[30] J. Xie, W. J. Ng, L. Y. Lee, C. Wang, *J. Colloid Interface Sci.* **2008**, *317*, 469.
[31] Z. Ahmad, H. B. Zhang, U. Farook, M. Edirisinghe, E. Stride, P. Colombo, *J. R. Soc., Interface* **2008**, *5*, 1255.
[32] M. Rasekh, Z. Ahmad, R. Cross, J. Hernandez-Gil, J. D. E. T. Wilton-Ely, P. W. Miller, *Mol. Pharm.* **2017**, *14*, 2010.
[33] A. Smeets, Clasen, G. Van der Mooter, *Eur. J. Pharm. Biopharm.* **2017**, *119*, 114.
[34] C. Larriba-Andaluz, J. F. de la Mora, *Phys. Fluids* **2010**, *22*, 072002.
[35] A. J. Kelly, *Aerosol Sci. Technol.* **1990**, *12*, 526.
[36] N. Bock, T. R. Dargaville, M. A. Woodruff. *Prog. Polym. Sci.* **2012**, *37*, 1510.
[37] O. Husain, W. Lau, M. Edirisinghe, M. Parhizkar, *Mater. Sci. Eng. C* **2016**, *65*, 240.
[38] S. N. Jayasinghe, M. J. Edirisinghe, *J. Aerosol Sci.* **2002**, *33*, 1379.
[39] M. Jafari-Nodoushan, J. Barzin, H. Mobedi, *Polym. Adv. Technol.* **2015**, *26*, 502.
[40] Y. Wu, A. Duong, L. L. James, B. E. Wyslouzil, in *The Delivery of Nanoparticles* (Ed: A. A. Hashim), InTech, Rijeka **2012**, pp. 223–242.

[41] H. Moghadam, M. Samimi, A. Samimi, M. Khorram, *Chem. Eng.* **2009**, *6*, 88.
[42] Y. Liu, J. He, J. Yu, H. Zeng, *Polym. Int.* **2008**, *57*, 632.
[43] M. F. Hossain, R. Gong, M. Rigout, *J. Text. Inst.* **2015**, *107*, 1.
[44] A. Ganan-Calvo, *Phys. Rev. Lett.* **1997**, *79*, 217.
[45] A. Ganan-Calvo, J. Davila, A. Barrero, *J. Aerosol Sci.* **1997**, *28*, 249.
[46] A. Barrero, A. Ganan-Calvo, J. Davila, A. Palacio, E. Gomez-Gonzalez, *Phys. Rev. E* **1998**, *58*, 7309.
[47] A. Ganan-Calvo, J. Lasheras. *Phys. Fluids A* **1991**, *3*, 1207.
[48] A. Ganan-Calvo. *J. Electrostat.* **1995**, *143*, 61.
[49] A. Ganan-Calvo, *J. Aerosol Sci.* **1999**, *30*, 863.
[50] J. Lopez-Herrera, A. Ganan-Calvo, M. Perez-Saborid, *J. Aerosol Sci.* **1999**, *30*, 895.
[51] A. Barrero, A. Ganan-Calvo, J. Davila, A. Palacios, E. Gomez-Gonzalez, *J. Electrostat.* **1999**, *47*, 13.
[52] A. Ganan-Calvo, *J. Fluid Mech.* **2004**, *507*, 203.
[53] C. U. Yurteri, R. P. A. Hartman, J. C. M. Marijnissen, *KONA Powder Part. J.* **2010**, *28*, 91.
[54] R. Sridhar, R. Lakshminarayanan, K. Madhaiyan, V. A. Barathi, K. H. C. Limh, S. Ramakrishna, *Chem. Soc. Rev.* **2015**, *44*, 790.
[55] D. N. Nguyen, C. Clasen, G. Van den Mooter, *J. Pharm. Sci.* **2016**, *105*, 2601.
[56] M. Zamani, M. P. Prabhakaran, E. S. Thian, S. Ramakrishna, *Int. J. Pharm.* **2014**, *473*, 134.
[57] A. Gomez, D. Bingham, L. de Juan, K. Tang, *J. Aerosol Sci.* **1998**, *29*, 561.
[58] A. A. K. Zarchi, S. Abbasi, M. A. Faramarzi, K. Gilani, M. Ghazi-Khansari, A. Amani, *Int. J. Biol. Macromol.* **2015**, *72*, 764.
[59] N. Yaghoobi, R. F. Majidi, M. A. Faramarzi, H. Baharifar, A. Amani, *Adv. Pharm. Bull.* **2017**, *7*, 131.
[60] H. F. Liu, J. M. Xi, H. M. Geng, G. B. Chen, Y. Zhu, S. S. Shi, Y. X. DOng, J. Cao, *Lat. Am. J. Pharm.* **2016**, *35*, 274.
[61] N. Hazeri, H. Tavanai, A. R. Moradi, *Sci. Technol. Adv. Mater.* **2012**, *13*, 035010.
[62] T. Suksamran, P. Opanasopit, T. Rojanarata, T. Ngawhirunpat, U. Ruktanonchai, P. Supaphol, *J. Microencapsul.* **2009**, *26*, 563.
[63] M. Rasekh, C. Young, M. Roldo, F. Lancien, J. Le Mevel, S. Hafizi, Z. Ahmad, E. Barbu, D. Gorecki, *J. Mater. Sci. Mater. Med.* **2015**, *26*, 256.
[64] M. G. Zeles-Hahn, Y. K. Lentz, T. J. Anchordoquy, C. S. Lengsfeld, *J. Electrostat.* **2011**, *69*, 67.
[65] Y. Lee, B. Wu, W. Zhuang, D. Chen, Y. J. Tang, *J. Microbiol. Methods* **2011**, *84*, 228.
[66] H. Park, P. Kim, T. Hwang, O. Kwon, T. Park, S. Choi, C. Yun, J. H. Kim, *Int. J. Pharm.* **2012**, *427*, 417.
[67] V. J. Venditto, E. E. Simanek, *Mol. Pharm.* **2010**, *7*, 307.
[68] Y. Wu, J. A. MacKay, J. R. McDaniel, A. Chilkoti, R. L. Clark, *Biomacromolecules* **2009**, *10*, 19.
[69] R. Cavalli, A. Bisazza, R. Bussano, M. Trotta, A. Civra, D. Lembo, E. Ranucci, P. Ferruti. *J. Drug Target.* **2011**, *2011*, 587604.
[70] M. Gulfam, J. Kim, J. M. Lee, B. Ku, B. H. Chung, B. G. Chung, *Langmuir* **2012**, *28*, 8216.
[71] S. Y. Lee, J. Lee, J. Park, J. Lee, S. Ko, J. Shim, J. Lee, M. Y. Heo, D. Kim, H. Cho. **2016**, *145*, 267.
[72] E. Sayed, C. Karavasili, K. Ruparelia, R. Haj-Ahmad, G. Charalambopoulou, T. Steriotis, D. Giasafaki, P. Cox, N. Singh, L. P. Giassafaki, A. Mpenekou, C. Markopoulou, I. Vizirianakis, M. W. Chang, D. Fatouros. *Z. Ahmad, J. Control. Release*. **2018**, *278*, 142.
[73] A. Bohr, J. Kristensen, M. Dyas, M. Edirisinghe, E. Stride. *J. R. Soc., Interface* **2012**, *9*, 2437.
[74] F. Delie, M. Berton, E. Allemann, R. Gurny, *Int. J. Pharm.* **2001**, *214*, 25.
[75] F. Tewes, E. Munnier, B. Antoon, L. N. Okassa, S. Cohen-Jonathan, H. Marchais, L. Douziech-Eyrolles, M. Souce, P. Dubois, I. Chourpa, *Eur. J. Pharm. Biopharm.* **2007**, *66*, 488.
[76] A. Bohr, J. P. Boetker, T. Rades, J. Rantanen, M. Yang, *Curr. Pharm. Des.* **2014**, *20*, 325.
[77] M. Nyström, J. Roine, M. Murtomaa, R. M. Sankaran, H. A. Santos, J. Salonen, *Eur. J. Pharm. Biopharm.* **2015**, *89*, 182.
[78] O. Mustapha, F. U. Din, D. W. Kim, J. H. Park, K. B. Woo, S. Lim, Y. S. Youn, K. H. Cho, R. Rashid, A. M. Yousaf, J. O. Kim, C. S. Yong, H. Choi, *J. Microencapsul.* **2016**, *33*, 323.
[79] A. K. Jain, V. Sood, M. Bora, R. Vasita, D. S. Katti, *Carbohydr. Polym.* **2014**, *112*, 225.
[80] G. Johannesson, E. Stefansson, T. Loftsson, *Dev. Ophthalmol.* **2016**, *55*, 93.
[81] R. A. Schwendener, *Ther. Adv. Vaccines* **2014**, *2*, 159.
[82] P. Deshpande, S. Biswas, V. P. Torchilin, *Nanomedicine* **2013**, *8*, 1509.
[83] A. Danion, H. Brochu, Y. Martin, P. Vermette. *J. Biomed. Mater. Res. A* **2007**, *82A*, 41.
[84] D. G. Yu, J. H. Yang, X. Wang, F. Tian, *Nanotechnology* **2012**, *23*, 105606.
[85] M. P. Prabhakaran, M. Zamani, B. Felice, S. Ramakrishna. *Mat. Sci. Eng. C* **2015**, *56*, 66.
[86] F. Imanparast, M. A. Faramarzi, M. Paknejad, F. Kobarfard, *J. Appl. Polym. Sci.* **2016**, *133*, 43602.
[87] P. Mehta, L. Justo, S. Walsh, M. S. Arshad, C. G. Wilson, C. K. O'Sullivan, S. M. Moghimi, I. S. Vizirianakis, K. Avgoustakis, D. G. Fatouros, Z. Ahmad, *J. Drug Target.* **2015**, *23*, 305.
[88] A. S. Qayyum, E. Jain, G. Kolar, Y. Kim, S. A. Sell, S. P. Zustiak, *Biofabrication* **2017**, *9*, 025019.
[89] C. Mu, X. Li, J. Guo, C. Bi, D. Li, *J. Appl. Polym. Sci.* **2013**, *129*, 773.
[90] W. A. K. Mahmood, M. H. Azarian, W. F. B. W. Fathilah, E. Kwok, *J. Appl. Polym. Sci.* **2017**, *134*, 45048.
[91] K. Hayashi, K. Ono, H. Suzuki, M. Sawada, M. Moriya, W. Sakamoto, T. Yogo, *Small* **2010**, *6*, 2384.
[92] L. Hia, P. Pasbakhsh, E. S. Chan, S. P. Chai, *Sci. Rep.* **2016**, *6*, 34674.
[93] P. Sofokleous, W. K. Lau, M. J. Edirisinghe, E. Stride, *RSC Adv.* **2016**, *6*, 75258.
[94] Y. Gao, D. Zhao, M. W. Chang, Z. Ahmad, X. Li, H. Suo, J. S. Li, *Mater. Lett.* **2015**, *146*, 59.
[95] A. M. Nikoo, R. Kadkhodaee, B. Ghorani, H. Razzaq, N. Tucker, *J. Microencapsul.* **2016**, *33*, 605.
[96] Y. Guan, Y. Zhou, J. Sheng, Z. Y. Jiang, H. Jumahan, Y. Hu, *J. Chem. Technol. Biotechnol.* **2016**, *91*, 1128.
[97] I. G. Loscertales, A. Barrero, I. Guerrero, R. Cortijo, M. Marquez, A. M. Ganan-Calvo, *Science* **2002**, *295*, 1695.
[98] X. P. Chen, L. B. Jia, X. Z. Yin, J. S. Cheng, J. Lu, *Phys. Fluids.* **2005**, *17*, 032101.
[99] M. Marlais, R. J. Coward, *Pediatr. Nephrol.* **2015**, *30*, 1217.
[100] S. Kim, H. Lee, S. Cho, J. Park, J. Park, J. Hwane, *Ind. Eng. Chem. Res.* **2011**, *50*, 13762.
[101] X. Li, Y. Liu, J. Zhang, J. Qu, M. Li, *Mater. Sci. Eng. C* **2017**, *72*, 394.
[102] N. Laelorspoen, S. Wongsasulak, T. Yoovidhya, S. Devahastin, *J. Funct. Foods* **2014**, *7*, 342.
[103] P. Pitigraisorn, K. Srichaisupakit, N. Wongpadungkiat, S. Wongsasulak, *J. Food Eng.* **2017**, *192*, 11.
[104] D. N. Nguyen, L. Palangetic, C. Clasen, G. Van de Mooter, *J. Pharm. Pharmacol.* **2016**, *68*, 625.
[105] S. Sakuma, S. Matsumoto, N. Ishizuka, K. Mohri, M. Fukushima, C. Ohba, K. Kawakami, *J. Pharm. Sci.* **2015**, *104*, 2977.
[106] C. C. Chuang, K. Martinez, G. Xie, A. Kennedy, A. Bumrungpert, A. Overman, W. Jia, M. K. McIntosh, *Am. J. Clin. Nutr.* **2010**, *92*, 1511.
[107] C. Li, D. Yu, G. R. Williams, Z. Wang, *PLoS One* **2014**, *9*, 1.
[108] J. W. Xie, J. C. M. Marijnissen, C. H. Wang, *Biomaterials* **2006**, *27*, 3321.

[109] H. N. Ho, I. Laidmae, K. Kogermann, A. Lust, A. Meos, C. N. Nguyen, J. Heinamaki, *Drug Dev. Ind. Pharm.* **2017**, *43*, 1134.
[110] M. Wang, Y. Wang, E. Omari-Siaw, S. Wang, Y. Zhu, X. Xu, *J. Pharm. Sci.* **2016**, *105*, 2427.
[111] S. Ghayempour, S. M. Mortazavi, *J. Electrostat.* **2013**, *71*, 717.
[112] M. Chang, E. Stride, M. Edirisinghe. *Soft Matter* **2009**, *5*, 5029.
[113] M. W. Chang, E. Stride, M. Edirisinghe. *J. R. Soc. Interface* **2010**, *6*, 5451.
[114] J. Xie, L. K. Lim, Y. Phua, J. Hua, C. Wang, *J. Colloid Interface Sci.* **2006**, *302*, 103.
[115] Y. Cao, B. Wang, Y. Wang, D. Lou, *RSC Adv.* **2014**, *4*, 30430.
[116] M. Rasekh, C. Young, M. Roldo, F. Lancien, J. Le Mevel, S. Hafizi, Z. Ahmad, E. Barbu, D. Gorecki. *J. Mater. Sci.* **2015**, *26*, 256.
[117] S. Hao, B. Wang, Y. Wang, *Mater. Sci. Eng. C* **2015**, *49*, 51.
[118] Y. Cao, B. Wang, Y. Wang, D. Lou, *J. Pharm. Sci.* **2014**, *103*, 3205.
[119] H. Lin, J. Chen, C. Chen, *Med. Biol. Eng. Comput.* **2016**, *54*, 1317.
[120] U. Farook, H. B. Zhang, M. J. Edirisinghe, E. Stride, N. Saffari, *Med. Eng. Phys.* **2007**, *29*, 749.
[121] U. Farook, E. Stride, M. J. Edirisinghe, *J. R. Soc. Interface* **2009**, *6*, 271.
[122] M. Parhizkar, E. Stride, M. J. Edirisinghe, *Lab Chip* **2014**, *14*, 2437.
[123] J. M. Zhang, E. Q. Li, S. T. Thoroddsen, *J. Micromech. Microeng.* **2014**, *24*, 035008.
[124] Y. Li, J. Li, H. B. Zhang, Y. S. Su, *Int. Conf. Biomed. Eng. Inf. 3rd.*, Sanya, China, May **2008**. https://doi.org/10.1109/BMEI.2008.200
[125] G. Li, T. Si, X. Luo, R. Xu, *Multimodal Biomedical Imaging XIII* **2014**, *8937*, 8937.
[126] S. Mahaingam, M. B. J. Meinders, M. Edirisinghe, *Langmuir* **2014**, *30*, 6694.
[127] Z. Ekemen, Z. Ahmad, E. Stride, D. Kaplan, M. Edirisinghe, *Biomacromolecules* **2013**, *14*, 1412.
[128] Z. Ekemen, H. Chang, Z. Ahmad, C. Bayram, Z. Rong, E. B. Denkbas, E. Stride, P. Vadgama, M. Edirisinghe, *Biomacromolecules* **2011**, *12*, 4291.
[129] W. Yan, X. J. Ong, K. T. Pun, D. Y. Tan, V. K. Sharma, Y. W. Tong, C. Wang, *Chem. Eng. J.* **2017**, *307*, 168.
[130] W. C. Yan, Q. W. Chua, X. J. Ong, V. K. Sharma, Y. W. Tong, C. H. Wang, *J. Colloid Interface Sci.* **2017**, *501*, 282.
[131] A. P. Kishan, E. M. Cosgriff-Hernandez, *J. Biomed. Mat. Res. Part A* **2017**, *105*, 2892.
[132] B. Son, B. Yeom, S. Song, C. Lee, T. S. Hwang, *J. Appl. Polym. Sci.* **2009**, *111*, 2892.
[133] R. Khajavi, M. Abbasipour, A. Bahador, *J. Appl. Polym. Sci.* **2015**, *133*, 42883.
[134] W. Xu, A. Atala, J. J. Yoo, S. J. Lee, *Biomed. Mater.* **2013**, *8*, 014104.
[135] J. Zeng, A. Aigner, F. Czubayko, T. Kissel, J. H. Wendorff, A. Greiner, *Biomacromolecules* **2005**, *6*, 1484.
[136] F. Ozcan, S. Ertul, E. Maltas, *Mater. Lett.* **2016**, *182*, 359.
[137] M. Li, M. J. Mondrinos, X. Chen, P. I. Lelkes, *IEEE/EMBS Med. Biol.* **2005**, *6*, 5858.
[138] X. Fang, D. H. Reneker, *J. Macromol. Sci., B* **1997**, *36*, 169.
[139] L. M. Bellan, J. D. Cross, E. A. Strychalski, J. Moran-Mirabal, H. G. Craighead, *Nano Lett.* **2006**, *6*, 2526.
[140] Y. K. Luu, K. Kim, B. S. Hsiao, B. Chu, M. Hadjiargyrou, *J. Controlled Release* **2003**, *89*, 341.
[141] T. Tokatlian, T. Segura, *Wiley Interdiscip. Rev. Nanomed. Nanobiotechnol.* **2010**, *2*, 305.
[142] W. W. Grabow, L. Jaeger, *Acc. Chem. Res.* **2014**, *47*, 1871.
[143] H. Cao, X. Jiang, C. Chai, S. Y. Chew, *J. Controlled Release* **2010**, *144*, 203.
[144] P. Rujitanaroj, Y. Wang, J. Wang, S. Y. Chew, *Biomaterials* **2011**, *32*, 5915.
[145] J. Xie, R. S. Tan, C. Wang, *J. Biomed. Mater. Res. A* **2008**, *85A*, 897.
[146] J. Xie, C. Wang, *Pharm. Res.* **2006**, *23*, 1817.
[147] X. L. Xu, L. X. Yang, X. Y. Xu, X. Wang, X. S. Chen, Q. Z. Liang, J. Zeng, X. B. Jing, *J. Controlled Release* **2005**, *108*, 33.
[148] X. Xu, X. Zhuang, X. Chen, X. Wang, L. Yang, X. Jing, *Macromol. Rapid Commun.* **2006**, *27*, 1637.
[149] Z. Zhang, S. Liu, H. Xiong, X. Jing, Z. Xie, X. Chen, Y. Huang, *Acta Biomater.* **2015**, *26*, 115.
[150] D. S. Katti, K. W. Robinson, F. K. Ko, C. T. Laurencin, *J. Biomed. Mater. Res.* **2004**, *70B*, 286.
[151] A. Toncheva, D. Paneva, V. Maximova, N. Manolova, I. Rashkov, *Eur. J. Pharm. Sci.* **2012**, *47*, 642.
[152] S. Zupancic, S. Sinha-Ray, S. Sinha-Ray, J. Kristl, A. L. Yarin, *Mol. Pharm.* **2016**, *13*, 295.
[153] S. E. Gilchrist, D. Lange, K. Letchford, H. Bach, L. Fazli, H. M. Burt, *J. Controlled Release* **2013**, *170*, 64.
[154] H. Liu, X. Ding, G. Zhou, P. Li, X. Wei, Y. Fan, *J. Nanomater.* **2013**, *2013*, 495708.
[155] S. Liao, R. Murugan, C. K. Chan, S. Ramakrishna, *J. Mech. Behav. Biomed. Mater.* **2008**, *1*, 252.
[156] A. S. Khan, Z. Ahmad, M. J. Edirisinghe, F. S. Wong, I. U. Rehman, *Acta Biomater.* **2008**, *4*, 1275.
[157] S. M. Zakaria, Z. S. H. Sharif, M. R. Othman, J. A. Jansen, *J. Biomed. Mater. Res. A.* **2013**, *101A*, 1977.
[158] C. Karavasili, N. Bouropoulos, I. Kontopoulou, A. Smith, S. M. Van der Merwe, I. Ur Rehman, Z. Ahmad, D. G. Fatouros, *J. Biomed. Mater. Res. A.* **2014**, *102*, 2583.
[159] M. Dash, F. Chiellini, R. M. Ottenbrite, E. Chiellini, *Prog. Polym. Sci.* **2011**, *36*, 981.
[160] J. A. Matthews, G. E. Wnek, D. G. Simpson, G. L. Bowlin, *Biomacromolecules*, **2002**, *3*, 232.
[161] J. Chen, G. Chang, J. Chen, *Colloids Surf. A* **2008**, *313–314*, 183.
[162] S. J. Lee, D. N. Heo, J. Moon, H. N. Park, W. Ko, M. S. Bae, J. B. Lee, S. W. Park, E. Kim, C. H. Lee, B. Jung, I. K. Kwon, *J. Nanosci. Nanotechnol.* **2014**, *14*, 7488.
[163] W. Li, T. Luo, Y. Shi, Y. Yang, X. Huang, K. Xing, L. Liu, M. Wang, *Integr. Ferroelectr.* **2014**, *151*, 164.
[164] J. Hu, F. Zeng, J. Wei, Y. Chen, Y. Chen, *J. Biomater. Sci., Polym. Ed.* **2014**, *25*, 257.
[165] W. Li, T. Luo, Y. Yang, X. Tan, L. Lui, *Langmuir* **2015**, *31*, 5141.
[166] D. Srinath, S. Lin, D. K. Knight, A. S. Rizkalla, K. Mequanint, *Tissue Eng. Regen. Med.* **2012**, *8*, 578.
[167] Gagandeep, T. Garg, B. Malik, G. Rath, A. K. Goyal, *Eur. J. Pharm. Sci.* **2014**, *53*, 10.
[168] Li, X., Wang, X., D. G. Yu, S. Ye, Q. Kuang, Q. Yi, X. Yao, *J. Nanomater.* **2012**, *2012*, 1.
[169] C. Huang, S. J. Soenen, E. van Gulck, J. Rejman, G. Vanham, B. Lucas, B. Geers, K. Braeckmans, V. Shahin, P. Spanoghe, J. Demeester, S. C. De Smedt, *Polym. Adv. Technol.* **2014**, *25*, 827.
[170] M. A. Collier, M. D. Gallovic, E. M. Bachelder, C. D. Sykes, A. Kashuba, K. M. Ainslie, *Pharm. Res.* **2016**, *33*, 1998.
[171] H. M. Borteh, M. D. Gallovic, S. Sharma, K. J. Peine, S. Miao, D. J. Brackman, K. Gregg, Y. Xu, X. Guo, J. Guan, E. M. Bachelder, K. M. Ainslie, *Langmuir* **2013**, *29*, 7957.
[172] H. Qu, S. Wei, Z. Guo, *J. Mater. Chem. A* **2013**, *1*, 11513.
[173] R. Khajavi, M. Abbasipour, *Sci. Iran.* **2012**, *19*, 2029.
[174] S. Chakraborty, I. Liao, A. Adler, K. W. Leong, *Adv. Drug Delivery Rev.* **2009**, *61*, 1043.
[175] T. Jarusuwannapoom, W. Hongroijanawiwat, S. Jitjaicham, L. Wannatong, M. Nithitanakul, C. Pattamaprom, P. Koombhongse, R. Rangkupan, P. Supaphol, *Eur. Polym. J.* **2005**, *41*, 409.
[176] S. Iqbal, M. H. Rashid, A. S. Arbab, M. Khan, *J. Biomed. Nanotechnol.* **2017**, *13*, 355.
[177] D. Han, X. Yu, Q. Chai, N. Ayres, A. J. Steckl, *ACS Appl. Mater. Interfaces* **2017**, *9*, 11858.

[178] E. Shoba, R. Lakra, M. S. Kiran, P. S. Korrapati, *Biomed. Mater.* **2017**, *12*, 1.
[179] H. Chen, Y. Peng, S. Wu, L. P. Tan, *Materials* **2016**, *9*, 272.
[180] G. Yang, J. Wang, Y. Wang, L. Li, X. Guo, S. Zhou, *ACS Nano* **2015**, *9*, 1161.
[181] E. Yan, Y. Fan, Z. Sun, J. Gao, X. Hao, S. Pei, C. Wang, L. Sun, D. Zhang, *Mat. Sci. Eng. C* **2014**, *41*, 217.
[182] H. Huang, C. He, H. Wang, X. Mo, *J. Biomed. Mater. Res. A* **2009**, *90A*, 1243.
[183] H. Park, H. H. Yoo, T. Hwang, T. Park, D. Paik, *J. Pharm. Invest.* **2012**, *42*, 89.
[184] Z. M. Huang, C. L. He, A. Z. Yang, Y. Z. Zhang, X. J. Hang, J. L. Yin, Q. S. Wu, *J. Biomed. Mater. Res. A* **2006**, *77A*, 169.
[185] M. He, H. Jiang, R. Wang, Y. Xie, C. Zhao, *J. Colloid Interface Sci.* **2017**, *490*, 270.
[186] C. L. He, Z. M. Huang, X. J. Han, L. Liu, H. S. Zhang, L. S. Chen, *J. Macromol. Sci., B* **2006**, *45*, 515.
[187] Y. Jiang, H. Mo, D. Yu, *Int. J. Pharm.* **2012**, *438*, 232.
[188] X. Li, Y. Li, D. Yu, Y. Liao, X. Wang, *Int. J. Mol. Sci.* **2013**, *14*, 21647.
[189] W. Huang, T. Zou, S. Li, J. Jing, X. Xia, X. Liu, *AAPS PharmSciTech.* **2013**, *14*, 675.
[190] W. Qian, D. Yu, Y. Li, X. Li, Y. Liao, X. Wang, *J. Nanomater.* **2013**, *2013*, 826471.
[191] D. Jia, Y. Gao, G. R. Williams, *Int. J. Pharm*. **2017**, *523*, 376.
[192] A. Raheja, A. Agarwal, V. Muthuvijayan, T. S. Chandra, T. S. Natarajan, *J. Biomater. Tissue Eng.* **2013**, *3*, 669.
[193] Y. Su, Q. Su, W. Liu, G. Jin, X. Mo, S. Ramakrishna, *J. Biomater. Sci., Polym. Ed.* **2012**, *23*, 861.
[194] P. Wen, K. Feng, H. Yang, X. Huang, M. Zong, W. Lou, *Carbohydr. Polym.* **2017**, *169*, 157.
[195] B. Wang, H. Zheng, M. W. Chang, Z. Ahmad, J. S. Li, *Colloids Surf. B: Biointerfaces* **2016**, *145*, 757.
[196] C. Gualandi, P. Torricelli, S. Panzavolta, S. Pagani, M. L. Focarete, A. Bigi, *Biomed. Mater.* **2016**, *11*, 025007.
[197] P. Boodagh, D. Guo, N. Nagiah, W. Tan, *J. Biomater. Sci., Polym. Ed.* **2016**, *27*, 1086.
[198] N. Lavielle, A. Hébraud, G. Schlatter, L. Thöny-Meyer, R. M. Rossi, A. M. Popa, *ACS Appl. Mater. Interfaces* **2013**, *5*, 10090.
[199] M. Roso, A. Lorenzetti, C. Boaretti, M. Modesti, *J. Nanomater.* **2016**, *2016*, 1.
[200] F. Hejazi, H. Mirzadeh. *J. Mat. Sci.* **2016**, *27*, 143.
[201] L. Francis, J. Venugopal, M. P. Prabhakaran, V. Thavasi, E. Marsano, S. Ramakrishna. *Acta Biomater*. **2010**, *6*, 4100.
[202] H. Bae, J. Lee. *J. Ind. Eng. Chem.* **2016**, *40*, 99.
[203] J. Park, M. Hardy, S. J. Kang, K. Barton, K. Adair, D. K. Mukhopadhyay, C. Y. Lee, M. S. Strano, A. G. Alleyne, J. G. Georgiadis, P. M. Ferreira, J. A. Rogers, *Nat. Mater*. **2007**, *6*, 782.
[204] C. H. Chen, D. A. Saville, I. A. Aksay, *Appl. Phys. Lett.* **2006**, *88*, 1.
[205] Y. Han, J. Dong, *J. Micromech. Microeng.* **2017**, *27*, 1.
[206] H. Lee, B. Seong, J. Kim, Y. Jang, D. Byun, *Small* **2014**, *10*, 3918.
[207] D. Youn, S. Kim, Y. Yang, S. Lim, S. Kim, S. Ahn, H. Sim, S. Ryu, D. Shin, J. Yoo, *Appl. Phys. A* **2009**, *96*, 933.
[208] D. Lee, Y. Shin, S. Park, T. Yu, J. Hwang, *Appl. Phys. Lett.* **2007**, *90*, 081905.
[209] K. Wang, M. D. Paine, J. P. W. Stark, *J. Appl. Phys.* **2009**, *106*, 024907.
[210] Y. Kim, S. Jang, J. H. Oh, *Appl. Phys. Lett.* **2015**, *106*, 014103.
[211] K. Wang, M. D. Paine, J. P. W. Stark, *Optoelectron. Adv. Mater. Rapid Commun.* **2010**, *4*, 365.
[212] K. Rahman, A. Khan, N. M. Muhammad, J. Jo, K. Choi, *J. Micromech. Microeng.* **2012**, *22*, 065012.
[213] H. Qin, J. Dong, Y. Lee, *Robot. Comput. Integrated Manuf.* **2017**, *43*, 179.
[214] A. Khan, K. Rahman, D. S. Kim, K. H. Choi, *J. Mater. Process. Technol.* **2012**, *212*, 700.
[215] K. Wang, J. P. W. Stark, *J. Nanoparticle Res.* **2010**, *12*, 707.
[216] S. R. Samarasinghe, I. Pastoriza-Santos, M. J. Edirisinghe, M. J. Reece, L. M. Liz-Marzan, *Gold Bulletin* **2006**, *39*, 48.
[217] E. S. Thian, J. Huang, Z. Ahmad, M. J. Edirisinghe, S. N. Jayasinghe, D. C. Ireland, R. A. Brooks, N. Rushton, S. M. Best, W. Bonfield, *J. Biomed. Mater. Res. A* **2008**, *85A*, 188.
[218] K. Shigeta, Y. He, E. Sutanto, S. Kang, A. Le, R. G. Nuzzo, A. G. Alleyne, P. M. Ferreira, Y. Lu, J. A. Rogers, *Anal. Chem.* **2012**, *84*, 10012.
[219] H. Kim, D. Lee, J. Park, J. Kim, J. Hwang, H. Jung, *Exp. Tech.* **2007**, *31*, 15.
[220] Z. Ahmad, J. Huang, M. J. Edirisinghe, S. N. Jayasinghe, S. M. Best, W. Bonfield, R. A. Brooks, N. Rushton, *J. Biomed. Nanotechnol.* **2006**, *2*, 201.
[221] Y. Zhu, Y. Chen, G. Xu, X. Ye, D. He, J. Zhong, *Mater. Sci. Eng. C* **2012**, *32*, 390.
[222] M. Kim, H. Yun, G. H. Kim, *Sci. Rep*. **2017**, *7*, 3166.
[223] D. Z. Wang, M. J. Edirisinghe, S. N. Jayasinghe, *J. Am. Ceram. Soc.* **2006**, *89*, 1727.
[224] A. Gupta, A. M. Seifalian, Z. Ahmad, M. J. Edirisinghe, M. C. Winslet, *J. Bioact. Compat. Polym.* **2007**, *22*, 265.
[225] M. Rasekh, Z. Ahmad, R. Day, A. Wickham, M. Edirisinghe, *Adv. Eng. Mater.* **2011**, *13*, B296.
[226] J. Wang, M. Chang, Z. Ahmad, J. Li, *J. Drug Delivery Sci. Technol.* **2016**, *35*, 114.
[227] X. Wang, Y. Wang, K. Wei, N. Zhao, S. Zhang, J. Chen, *J. Mater. Process. Technol.* **2009**, *209*, 348.
[228] J. Wang, H. Zheng, M. W. Chang, Z. Ahmad, J. S. Li, *Sci. Rep*. **2017**, *7*, 43924.
[229] Z. Wang, X. Chen, J. Zeng, F. Liang, P. Wu, H. Wang, *AIP Adv*. **2017**, *7*, 035310.
[230] A. Khalf, K. Singarapu, S. V. Madihally. *React. Funct. Polym.* **2015**, *90*, 36.
[231] S. Labbaf, S. Deb, G. Cama, E. Stride, M. Edirisinghe, *J. Colloid Interface Sci.* **2013**, *409*, 245.
[232] S. Labbaf, H. Ghanbar, E. Stride, M. Edirisinghe, *Macromol. Rapid Commun.* **2014**, *35*, 618.
[233] Y. Lee, M. Bai, D. Chen, *Colloids Surf. B.* **2011**, *82*, 104.
[234] C. Zhang, Z. Yao, Q. Ding, J. J. Choi, Z. Ahmad, M. Chang, J. Li, *ACS Appl. Mater. Interfaces* **2017**, *9*, 21485.
[235] J. D. Regele, M. J. Papac, M. J. A. Rickard, D. Dunn-Rankin, *J. Aerosol Sci.* **2002**, *33*, 1471.
[236] S. Jiang, G. Duan, E. Zussman, A. Greiner, S. Agarwal, *ACS Appl. Mater. Interfaces* **2014**, *6*, 5918.
[237] W. Liu, C. Ni, D. B. Chase, J. F. Rabolt, *ACS Macro Lett.* **2013**, *2*, 466.
[238] D. Han, A. J. Steckl, *ACS Appl. Mater. Interfaces* **2013**, *5*, 8241.
[239] D. Han, S. Sherman, S. Filocamo, A. J. Steckl, *Acta Biomater.* **2017**, *53*, 242.
[240] J. Stark, B. Stevens, M. Kent, M. Sandford, M. Alexander, *J Spacecr. Rockets* **2005**, *42*, 628.
[241] W. Deng, J. K. Klemic, X. Li, M. A. Reed, A. Gomez, *J. Aerosol Sci.* **2006**, *37*, 696.
[242] L. Licklider, X. Q. Wang, A. Desai, Y. C. Tai, T. D. Lee, *Anal. Chem.* **2000**, *72*, 367.
[243] B. Q. T. Si, D. Byun, S. Lee, *J. Aerosol Sci.* **2007**, *38*, 924.
[244] M. S. Lhernould, P. Lambert, *J. Electrostat.* **2011**, *69*, 313.
[245] Y. Yang, Z. Jia, Q. Li, L. Hou, J. Liu, L. Wang, Z. Guan, M. Zahn, *IEEE Trans. Dielectr. Electr. Insul.* **2010**, *17*, 1592.
[246] M. Parhizkar, P. J. T. Reardon, J. C. Knowles, R. J. Browning, E. Stride, R. B. Pedley, T. Grego, M. Edirisinghe, *Mater. Des.* **2017**, *126*, 73.
[247] H. Niu, T. Lin, *J. Nanomater.* **2012**, *2012*, 725950.

[248] J. H. Jordahl, S. Ramcharan, J. V. Gregory, J. Lahann. *Macromol. Rapid Commun.* **2017**, *38*, 1600437.
[249] A. L. Yarin, E. Zussman, *Polymer* **2004**, *142*, 1.
[250] X. Wang, H. Niu, T. Lin, X. Wang, *Polym. Eng. Sci.* **2009**, *49*, 1582.
[251] S. Tang, Y. Zeng, X. Wang, *Polym. Eng. Sci.* **2010**, *50*, 2252.
[252] H. Y. Chung, J. R. B. Hall, M. A. Gogins, D. G. Crofoot, T. M. Weik, US Patent 2004/0187454, **2004**.
[253] H. Y. Kim, *US Patent 6,991*, **2006**.
[254] A. L. Andrady, D. S. Ensor, T. A. Walker, P. Prabhu, *US Patent 7,591*,277, **2009**.
[255] L. Vyslouzilova, M. Buzgo, P. Pokorny, J. Chvojka, A. Mickova, M. Rampichova, J. Kula, K. Pejchar, M. Bilek, D. Lukas, E. Amler, *Int. J. Pharm.* **2017**, *516*, 293.
[256] K. M. Forward, A. Flores, G. C. Rutledge. *Chem. Eng. Sci.* **2013**, *104*, 250.
[257] R. Bocanegra, D. Galan, M. Marquez, I. G. Loscertales, A. Barrero, *J. Aerosol Sci.* **2005**, *36*, 1387.
[258] C. Zhang, M. Chang, Z. Ahmad, W. Hu, D. Zhao, J. Li, *RSC Adv*. **2015**, *5*, 87919.
[259] F. Mou, C. Chen, J. Guan, D. R. Chen, H. Jing, *Nanoscale* **2013**, *5*, 2055.
[260] S. Rahmani, C. H. Villa, A. F. Dishman, M. E. Grabowski, D. C. Pan, H. Durmaz, A. C. Misra, L. Colón-Meléndez, M. J. Solomon, V. R. Muzykantov, J. Lahann, *J. Drug Target.* **2015**, *23*, 750.
[261] C. Zhang, M. Chang, Y. Li, Y. Qi, J. Wu, Z. Ahmad, J. Li, *RSC Adv*. **2016**, *6*, 77174.
[262] H. Ueda, K. Takeuchi, A. Kikuchi, *J. Appl. Phys.* **2017**, *56*, 04CL05.
[263] H. Kim, S. S. Kim, *Aerosol Sci. Technol*. **2015**, *49*, 11.
[264] R. Haj-Ahmad, M. Rasekh, K. Nazari, K. Onaiwu, B. Yousef, S. Morgan, D. Evans, M.W. Chang, J. Hall, C. Samwell, Z. Ahmad, *Drug Delivery Trans. Res.* **2018**, 1. https://doi.org/10.1007/s13346-018-0518-4
[265] L. Li, Z. Jiang, Q. Pan, T. Fang, *J. Chem.* **2013**, *2013*, 508905.
[266] S. N. Jayasinghe, N. Suter, *Biomicrofluidics* **2010**, *4*, 014106.
[267] Wahyudiono, K. Murakami, S. Machmudah, M. Sasaki, M. Goto, *High Press. Res.* **2012**, *32*, 54.
[268] Wahyudiono, S. Machmudah, H. Kanda, S. Okubayashi, M. Goto, *Chem. Eng. Process* **2014**, *77*, 1.
[269] Wahyudiono, K. Okamoto, S. Machmudah, H. Kanda, M. Goto, *Polym. Eng. Sci.* **2016**, *56*, 752.
[270] H. Peng, Y. Liu, S. Ramakrishna, *J. Appl. Polym. Sci*. **2017**, *134*, 44578.
[271] L. Wang, Z. Ahmad, J. Huang, J. S. Li, M. W. Chang, *Chem. Eng. J.* **2017**, *330*, 541.
[272] L. Wang, M. Chang, Z. Ahmad, H. Zheng, J. Li, *Chem. Eng. J.* **2017**, *307*, 661.
[273] D. Edmondson, A. Cooper, S. Jana, D. Wood, M. Zhang, *J. Mater. Chem.* **2012**, *22*, 18646.
[274] M. Kancheva, A. Toncheva, N. Manolova, I. Rashkov, *Mater. Lett*. **2014**, *136*, 150.
[275] H. Chen, Y. Liu, Q. Hu, *Exp. Cell Res.* **2015**, *338*, 261.
[276] J. Stankus, J. Guan, K. Fujimoto, W. Wagner, *Biomaterials* **2006**, *27*, 735.
[277] J. J. Stankus, L. Soletti, K. Fujimoto, Y. Hong, D. A. Vorp, W. R. Wagner, *Biomaterials* **2007**, *28*, 2738.
[278] A. Townsend-Nicholson, S. N. Jayasinghe, *Biomacromolecules* **2006**, *7*, 3364.
[279] D. Poncelet, P. de Vos, N. Suter, S. N. Jayasinghe, *Adv. Healthcare Mater.* **2012**, *1*, 27.
[280] S. N. Jayasinghe, S. Irvine, J. R. McEwan, *Nanomedicine* **2007**, *2*, 555.
[281] S. N. Jayasinghe, *Analyst* **2013**, *138*, 2215.
[282] E. Ward, E. Chan, K. Gustafsson, S. N. Jayasinghe, *Analyst* **2010**, *135*, 1042.
[283] S. Arumuganathar, S. Irvine, J. R. McEwan, S. N. Jayasinghe, *Biomed. Mater.* **2007**, *2*, 211.
[284] E. Ehler, S. N. Jayasinghe, *Analyst* **2014**, *139*, 4449.
[285] L. Weidenbacher, A. Abrishamkar, M. Rottmar, A. G. Guex, K. Maniura-Weber, A. J. deMello, S. J. Ferguson, R. M. Rossi, G. Fortunato, *Acta Biomater.* **2017**, *64*, 137.
[286] H. Niu, X. Wang, T. Lin, *J. Eng. Fiber. Fabr.* **2012**, *45*, 17.
[287] Z. Ma, H. Ji, D. Tan, G. Dong, Y. Teng, J. Zhou, M. Guan, J. Qiu, M. Zhang, *Nanotechnology* **2011**, *22*, 305307.
[288] J. Zhang, T. Zheng, E. Alarcin, B. Byambaa, X. Guan, J. Ding, Y. S. Zhang, Z. Li, *Small* **2017**, *13*, 1701949.
[289] Y. Gao, T. W. Teoh, Q. Wang, G. R. Williams, *J. Mater. Chem. B* **2017**, *5*, 9165.